Towards Early Prenatal Diagnosis Using the Third Dimension

Hein Bogers

Financial support for printing of this thesis was provided by Erasmus University Rotterdam and the Department of Obstetrics and Gynaecology, Erasmus MC, University Medical Centre, Rotterdam

ISBN: 978-94-6361-177-0

Layout and Printing: Optima Grafische Communicatie (www.ogc.nl)

Towards Early Prenatal Diagnosis Using the Third Dimension

Op weg naar vroege prenatale diagnostiek
met behulp van de derde dimensie

Proefschrift

ter verkrijging van de graad van doctor aan de
Erasmus Universiteit Rotterdam
op gezag van de
rector magnificus

Prof. dr. R.C.M.E. Engels

en volgens besluit van het College voor Promoties.
De openbare verdediging zal plaatsvinden op

dinsdag 4 december 2018 om 13.30 uur

door

Hein Bogers
geboren te Gouda

Erasmus University Rotterdam

Promotiecommissie

Promotoren:	Prof. dr. E.A.P. Steegers
	Prof. dr. P.J. van der Spek
Overige leden:	Prof. dr. G.J. Kleinrensink
	Prof. dr. D. Tibboel
	Dr. E.J.O. Kompanje
Co-promotoren:	Dr. N. Exalto
	Dr. A.H.J. Koning

Paranimfen:	Drs. T.J. van den Berg
	Dr. T.F. Runia

Contents

CHAPTER 1

Introduction

Prenatal screening for congenital anomalies, using ultrasound techniques for the so called *structural anomaly scan,* is traditionally performed in the second trimester of pregnancy. Ultrasound is, as a non-invasive technique, of course preferred above exposure to ionising radiation. The technique improved significantly the last decades as well as the availability, both resulting in a broad clinical experience with this technique. Importantly, when the so-called *as low as reasonably practicable* (ALARP) principle is respected, ultrasound is generally regarded as a safe diagnostic instrument for both mother and child.[1]

Detecting congenital anomalies

Although the structural anomaly scan usually is scheduled in the second trimester of pregnancy, there is an increasing interest in the detection of structural abnormalities in the first trimester.[2-4] Nuchal translucency measurement - as part of the combined test - and technical improvement of ultrasound equipment, yielding an improved visualisation, have contributed to this shift of interest from the second to the first trimester. Early detection of abnormalities has great advantages compared to detection later in pregnancy. For instance, early prenatal diagnosis of congenital anomalies provides more time for physicians to counsel and more time for the patients to consider all treatment options, including termination of pregnancy.[5] There are however drawbacks, mainly caused by marked changing anatomy in the first trimester of pregnancy. To be able to diagnose abnormal development, a profound knowledge of the transforming anatomy of the developing human embryo is necessary. Although additional testing may enhance the detection rate of congenital anomalies and early prenatal screening may increase sensitivity, specificity may concurrently be decreased.[6] Therefore, familiarity with the specific sonographic appearance of normal development in early pregnancy is utmost important for optimising these test characteristics.

Third dimension

In daily obstetric practice, two-dimensional (2D) ultrasound is used to screen for and to diagnose congenital anomalies. 3D imaging has however multiple advantages over conventional 2D ultrasound. By obtaining a 3D

volume instead of a 2D plane, very precise localisation of structures can be achieved via the orthogonal triplanar image, which can help in confirming diagnoses.[7] Furthermore, surface-rendered 3D volumes provide the possibility to evaluate surface abnormalities and may aid in counselling future parents.[8, 9] By using special software, like Virtual Organ Computer-aided AnaLysis (VOCAL™; GE Medical Systems, Zipf, Austria) it is even possible to add the third dimension on a two-dimensional (2D) screen creating the opportunity to measure volumes.[10]

3D virtual reality

Recent developments in 3D techniques have resulted in improved imaging. A new visualisation approach allows 3D volumes to be translated into a Cartesian format to be displayed in a Cartesian coordinate system, like the BARCO I-Space (Barco N.V., Kortrijk, Belgium). The BARCO I-Space is based on a 3D virtual reality (VR) environment that allows depth perception and interaction with the ultrasound data in a more natural and intuitive way compared to 3D images displayed on a 2D screen. This 3D VR technique has already proved its value in obstetric ultrasonography, e.g., the determination of ambiguous genitalia in a later stage of pregnancy[11] and the evaluation of conjoined twins.[12] Also in a preclinical setting, 3D VR has given ample insight in the early development of extra-embryonal structures like the trophoblast/placenta[13, 14] and the umbilical cord, vitelline duct and yolk sac.[15] This technique additionally provides the possibility to obtain volume measurements being different in normal pregnancy[16, 17] and in aneuploid pregnancies[18] and therefore seems to be a promising innovation in prenatal diagnosis.

Aims and outline of this thesis

The general aim of research of this thesis was to better understand normal physiological changes of the developing human embryo by using novel imaging techniques, serving as a background for determining the difference between normal and abnormal development. We examined the sonographic appearance of the brain, midgut, genitalia, feet and the curvature in the first trimester of pregnancy by means of both 3D and 3D VR technology.

The following research objectives were defined:

1. To describe first trimester growth trajectories of the telecephalon, diencephalon and mesencephalon using 3D ultrasound. Compared to other organ systems, relatively little is known about cerebral development in utero.
2. To investigate the development of the physiological exomphalos using 3D VR. During normal development of the midgut in the first trimester, the intestines protrude into the umbilical cord causing an omphalocoele. Pathological omphalocoele is generally regarded as a major congenital anomaly and might be caused by its physiological counterpart failing to resolve.
3. To evaluate the development of the lower leg and foot during the period of transient 'physiological clubfoot' using 3D VR. A clubfoot (pes equinovarus) is a congenital anomaly with a relatively high incidence.
4. To investigate whether there is scientific basis for reliable sex determination at the end of the first trimester of pregnancy using 3D VR being the best available technique for studying embryonic surface development. Although the foetal genitalia have not been developed entirely at the end of the first trimester of pregnancy, several clinicians and authors report to be able to predict the sex of the baby at that moment.
5. To describe, for the first time, the development of the embryonic curvature using 3D ultrasound. Additionally we investigated whether embryos from pregnancies resulting in a miscarriage have differences in the curvature compared to ongoing pregnancies.

The implications and limitations of this research, but also new opportunities, are discussed at the end of the thesis.

References

1. Houston LE, Odibo AO, Macones GA. The safety of obstetrical ultrasound: a review. Prenat Diagn. 2009;29(13):1204-12.
2. Syngelaki A, Chelemen T, Dagklis T, Allan L, Nicolaides KH. Challenges in the diagnosis of fetal non-chromosomal abnormalities at 11-13 weeks. Prenat Diagn. 2011;31(1):90-102.
3. Chaoui R, Nicolaides KH. Detecting open spina bifida at the 11-13-week scan by assessing intracranial translucency and the posterior brain region: mid-sagittal or axial plane? Ultrasound Obstet Gynecol. 2011;38(6):609-12.
4. Nicolaides KH. A model for a new pyramid of prenatal care based on the 11 to 13 weeks' assessment. Prenat Diagn. 2011;31(1):3-6.
5. Fong KW, Toi A, Salem S, Hornberger LK, Chitayat D, Keating SJ, et al. Detection of fetal structural abnormalities with US during early pregnancy. Radiographics. 2004;24(1):157-74.
6. Health Council of the Netherlands. Population Screening Act: first trimester scan for prenatal screening. The Hague: Health Council of the Netherlands, 2014; publication no. 2014/31.
7. Merz E, Abramowicz JS. 3D/4D ultrasound in prenatal diagnosis: is it time for routine use? Clin Obstet Gynecol. 2012;55(1):336-51.
8. Rubesova E, Barth RA. Advances in fetal imaging. Am J Perinatol. 2014;31(7): 567-76.
9. Anandakumar C, Nuruddin Badruddin M, Chua TM, Wong YC, Chia D. First-trimester prenatal diagnosis of omphalocele using three-dimensional ultrasonography. Ultrasound Obstet Gynecol. 2002;20(6):635-6.
10. Raine-Fenning NJ, Clewes JS, Kendall NR, Bunkheila AK, Campbell BK, Johnson IR. The interobserver reliability and validity of volume calculation from three-dimensional ultrasound datasets in the in vitro setting. Ultrasound Obstet Gynecol. 2003;21(3):283-91.
11. Verwoerd-Dikkeboom CM, Koning AH, Groenenberg IA, Smit BJ, Brezinka C, Van Der Spek PJ, et al. Using virtual reality for evaluation of fetal ambiguous genitalia. Ultrasound Obstet Gynecol. 2008;32(4):510-4.
12. Baken L, Rousian M, Kompanje EJ, Koning AH, van der Spek PJ, Steegers EA, et al. Diagnostic techniques and criteria for first-trimester conjoined twin documentation: a review of the literature illustrated by three recent cases. Obstet Gynecol Surv. 2013;68(11):743-52.

13. Reus AD, Klop-van der Aa J, Rifouna MS, Koning AH, Exalto N, van der Spek PJ, et al. Early pregnancy placental bed and fetal vascular volume measurements using 3-D virtual reality. Ultrasound Med Biol. 2014;40(8):1796-803.

14. Rifouna MS, Reus AD, Koning AH, van der Spek PJ, Exalto N, Steegers EA, et al. First trimester trophoblast and placental bed vascular volume measurements in IVF or IVF/ICSI pregnancies. Hum Reprod. 2014;29(12):2644-9.

15. Rousian M, Verwoerd-Dikkeboom CM, Koning AH, Hop WC, van der Spek PJ, Steegers EA, et al. First trimester umbilical cord and vitelline duct measurements using virtual reality. Early Hum Dev. 2011;87(2):77-82.

16. Verwoerd-Dikkeboom CM, Koning AH, Hop WC, van der Spek PJ, Exalto N, Steegers EA. Innovative virtual reality measurements for embryonic growth and development. Hum Reprod. 2010;25(6):1404-10.

17. Rousian M, Koning AH, van Oppenraaij RH, Hop WC, Verwoerd-Dikkeboom CM, van der Spek PJ, et al. An innovative virtual reality technique for automated human embryonic volume measurements. Hum Reprod. 2010;25(9):2210-6.

18. Baken L, van Heesch PN, Wildschut HI, Koning AH, van der Spek PJ, Steegers EA, et al. First-trimester crown-rump length and embryonic volume of aneuploid fetuses measured in virtual reality. Ultrasound Obstet Gynecol. 2013;41(5): 521-5.

CHAPTER 2

First trimester size charts of embryonic brain structures

Gijtenbeek M, Bogers H, Groenenberg IAL, Exalto N, Willemsen SP, Steegers EAP, Eilers PHC, Steegers-Theunissen RPM

Hum Reprod. 2014; 29(2): 201-7

Abstract

Study question: Can reliable size charts of human embryonic brain structures be created from three-dimensional ultrasound (3D US) visualisations?

Summary answer: Reliable size charts of human embryonic brain structures can be created from high-quality images.

What is known already: Previous studies on the visualisation of both the cavities and the walls of the brain compartments were performed using 2D-US, 3D US or invasive intrauterine sonography. However, the walls of the diencephalon, mesencephalon and telencephalon have not been measured non-invasively before. Last-decade improvements in transvaginal ultrasound techniques allow a better visualisation and offer the tools to measure these human embryonic brain structures with precision.

Study design, size, duration: This study is embedded in a prospective periconceptional cohort study. A total of 141 pregnancies were included before the sixth week of gestation and were monitored until delivery to assess complications and adverse outcomes.

Participants/materials, setting, methods: For the analysis of embryonic growth, 596 3D US scans encompassing the entire embryo were obtained from 106 singleton non-malformed live birth pregnancies between 7^{+0} and 12^{+6} weeks' gestational age (GA). Using 4D View (3D software) the measured embryonic brain structures comprised thickness of the diencephalon, mesencephalon and telencephalon, and the total diameter of the diencephalon and mesencephalon.

Main results and the role of chance: Of 596 3D scans, 161 (27%) high-quality scans of 79 pregnancies were eligible for analysis. The reliability of all embryonic brain structure measurements, based on the intra-class correlation coefficients (ICCs) (all above 0.98), was excellent. Bland–Altman plots showed moderate agreement for measurements of the telencephalon,

but for all other measurements the agreement was good. Size charts were constructed according to crown-rump length (CRL).

Limitations, reasons for caution: The percentage of high-quality scans suitable for analysis of these brain structures was low (27%).

Wider implications of the findings: The size charts of human embryonic brain structures can be used to study normal and abnormal development of brain development in future. Also, the effects of periconceptional maternal exposures, such as folic acid supplement use and smoking, on human embryonic brain development can be a topic of future research.

Introduction

The human brain is complex. During its rapid development it undergoes remarkable anatomical changes throughout pregnancy, even in the early first trimester of pregnancy. The detection of brain abnormalities by ultrasonography (US) during early pregnancy is therefore a challenge. In the first trimester the majority of structural anomalies detected by US comprise severe and lethal defects.[1] Recent studies suggest that periconceptional maternal exposures can affect the development of the human embryonic and foetal brain;[2, 3] however, the actual influence of these exposures remains unknown. Therefore, longitudinal studies investigating the growth of human embryonic brain structures might provide new insights.

In many countries, the structural anomaly scan is performed in the second trimester of pregnancy. However, first trimester detection of brain abnormalities has advantages compared with the detection in the second trimester of pregnancy, for example, it provides women more time for counselling and decision-making.[4] Early prenatal diagnosis requires, however, a profound knowledge of the anatomy of the developing human embryonic brain.

A first step is therefore to create size charts of human embryonic brain structures according to protocol, with validated non-invasive ultrasound techniques. During human embryonic brain development, the prosencephalon, mesencephalon and rhombencephalon can be distinguished at 5.5 weeks' gestational age (GA), as calculated from the first day of the last menstrual period (LMP). Between 6 and 8 weeks' GA, the prosencephalon divides into the telencephalon and diencephalon and the rhombencephalon divides into the metencephalon and myelencephalon.[5, 6]

Since the early 1990s, the availability of transvaginal high-velocity transducers with large apertures and/or annular array technology has offered the opportunity to perform studies on the visualisation of embryonic development with 2D-US and 3D US.[7-10] During the last decade, the human embryonic brain in particular has been a topic of interest in multiple studies.[1, 11, 12] Blaas et al. created growth trajectories from 7 weeks' GA onwards for the hemispheres of the telencephalon and for the fluid-filled vesicles of the diencephalon and mesencephalon.[13, 14] Tanaka et al. and Tanaka and Hata studied embryonic brain development using an intrauterine transducer for volume analysis of the fluid-filled brain cavities between 7 and 10 weeks' GA and for measurement of the embryonic brain mantle thickness between 6 and 11 weeks' GA.[11, 12]

The improvements in transvaginal ultrasound techniques over the last decade allow a better visualisation and offer the tools to measure these human embryonic brain structures with precision. Therefore, the aim of the present study was to create first trimester size charts of human embryonic brain structures in singleton non-malformed live birth pregnancies, using three-dimensional ultrasound (3D US) visualisation. We also determined the reliability of all measurements.

Study population and methods

Study population

This study is embedded in the Rotterdam Predict Study, a prospective periconceptional cohort study investigating the influence of gene–environment interactions and epigenetic mechanisms on reproductive parameters and (extra) embryonic and pregnancy outcome at the Erasmus MC University Hospital in Rotterdam, the Netherlands. Enrolment of pregnant women over 18 years of age, from the outpatient clinic of the Department of Obstetrics and Gynaecology, took place before the sixth week of gestation. In the Rotterdam Predict study, 3D ultrasound examinations were performed weekly between 6^{+0} and 12^{+6} weeks' GA, during which a series of 3D sweeps was obtained, encompassing the whole embryo.

In total, 141 pregnancies were monitored until delivery to assess complications and adverse outcomes. Non-participating patients/dropouts (n = 3), miscarriages (n = 16), terminations of pregnancy (n = 2), multiple pregnancies (n = 3), intrauterine foetal deaths/neonatal deaths (n = 2), congenital anomalies (n = 3) and pregnancies dated on crown-rump length (CRL) (n = 6) were excluded, leaving a total of 106 pregnancies eligible for the study.

GA was calculated according to the LMP, and in cases of an irregular menstrual cycle, unknown LMP or a discrepancy of >3 days, GA was determined by the CRL measurements performed in the first trimester. In case of conception by means of IVF or ISCI, the conception date was used to calculate the GA.

All pregnant patients gave written informed consent before participation. Approval of the study was obtained from the Central Committee for Human Research in The Hague and the local Medical Ethical and Institutional Review Board of the Erasmus MC, University Medical Centre in Rotterdam.

Measurements

The measurements were performed using a 4.5–11.9-MHz transvaginal probe of the Voluson E8 system (GE Medical Systems, Zipf, Austria). The stored 3D volumes were displayed in the orthogonal multiplanar mode using specialised 3D software (4D View, version 5.0, GE Medical Systems). The quality of the 3D volumes was evaluated off-line and only volumes without motion artefacts and with a clear demarcation of the borders of the brain structures were accepted for further analysis.

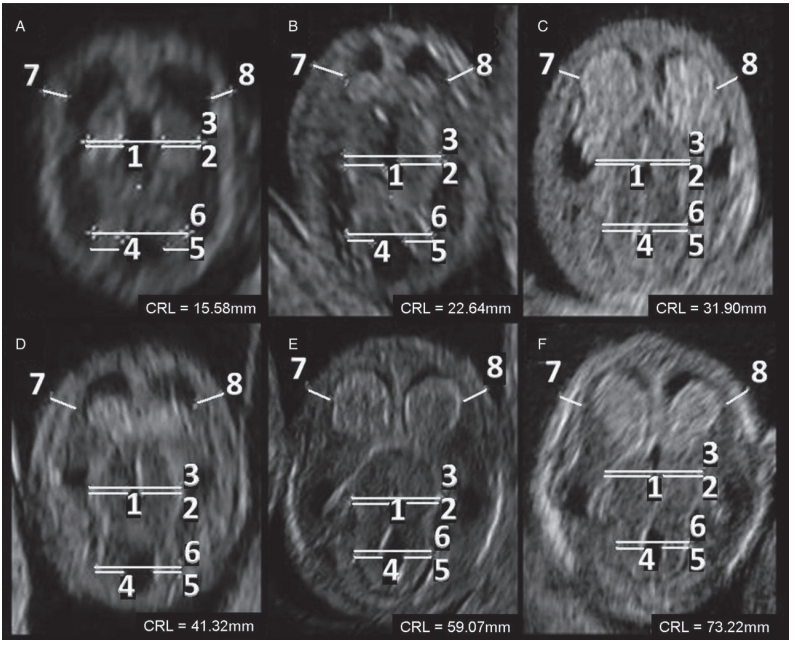

Figure 1: axial sections of the embryonic brain of embryos at 7–12 weeks' GA (A–F). The diencephalon thickness left (DTL; 1), diencephalon thickness right (DTR; 2), diencephalon total diameter (DTD; 3), mesencephalon thickness left (MTL; 4), mesencephalon thickness right (MTR; 5), mesencephalon total diameter (MTD; 6), telencephalon thickness left (TTL; 7) and telencephalon thickness right (TTR; 8) are measured using the 'distance two points' function. The respective CRL is shown in the image.

The following embryonic brain parameters were determined: left and right diencephalon thicknesses (DTL and DTR) and total diameter (DTD), left and right mesencephalon thicknesses (MTL and MTR) and total diameter (MTD) and left and right telencephalon thicknesses (TTL and TTR). According to a newly designed protocol, all measurements were performed in an axial or coronal section through the head of the embryo, with visualisation of the cavity of the diencephalon and mesencephalon (**Figure 1**). Measurements of the diencephalon and mesencephalon were performed by placing the callipers on the outer borders of these brain structures and the maximal thickness was measured. In the same axial plane also the cleavage of the telencephalic cavity, containing the choroid plexus, was visualised. In a line 45° from the longitudinal axis of the axial plane of the embryonic head, the diameters of the left and right lateral wall of the hemispheres of the telencephalon were measured.

All measurements in the same volume were independently repeated three times and the mean values were used for analysis. To assess intra- and inter-observer reproducibility, a randomly selected subset of 30 volumes from 30 randomly selected pregnancies was measured a second time by the same examiner (M.G.) and independently by another examiner (H.B.). For this purpose, five volumes were selected of each gestational week. Both examiners were blinded to the results of each other's measurements, each volume was unadjusted (raw data) and each measurement required manual adjustment of the volume to obtain the right image.

Statistical analysis

Using SPSS (Release 17.0 for Windows, IBM, USA), intra-class correlation coefficients (ICCs) were calculated to quantify the inter- and intra-observer reliability of the measurements. To assess the agreement between and within the two examiners Bland–Altman plots were created. The mean difference and mean percentage difference with corresponding 95% limits of agreement [mean (percentage) difference ± 1.96 SD] were calculated.[15]

We analysed the data cross-sectionally. We used the GAMLSS method[16] as implemented in R (version 2.15) to estimate percentile curves (P5, P50 and P95). We used a model that uses a spline to describe the trend, as a function of CRL, by P-splines. In all cases the logarithm (to base 10) of the measurements is taken as the dependent variable and a normal distribution of the variations around the trend is assumed. The logarithm of the standard deviation is allowed to change linearly with the CRL. The GAMLSS model specification formula is 'gamlss(*y* ~ps(crl), sigma.formula = ~ crl, family = 'NO')'. Here '*y*' is the logarithm of the size of the brain structure to be modelled.

Results

The mean age of the 106 pregnant patients was 32.4 years (SD: 4.91 years) and the mean BMI was 24.6 kg/m^2 (range: 19.1–38.3 kg/m^2). Fifty-five healthy girls and 51 healthy boys were born at a median GA of 39^{+4} weeks' GA (range: 26^{+5}–42^{+0} weeks' GA) with a median birthweight of 3378 g (range: 450–4700 g). A non-response analysis, comparing the characteristics between the pregnancies with (*n* = 79) and without measurable images (*n* = 27), did not show any significant differences. In gestational weeks 8

	Diencephalon	**Mesencephalon**	**Telencephalon**
Number of images	596	596	596
Number of measurements (%)	161 (27)	152 (26)	133 (22)
Number of patients with ≥1 measurement (%)	79 (75)	77 (73)	75 (71)
1 measurement (%)	40.5	41.6	52.0
2 measurements (%)	29.1	29.9	24.0
3 measurements (%)	16.5	18.2	10.6
4 measurements (%)	11.4	10.4	13.4
5 measurements (%)	2.5	0	0

Table 1: ultrasound data per brain structure for all included patients in the growth analysis (n = 106)

and 11, the embryonic brain structures of smaller embryos, according to CRL, were measured more often compared with bigger embryos ($P < 0.05$).

A total number of 596 3D US scans between 7^{+0} and 12^{+6} were performed in 106 patients, with an average number of 5.6 scans per patient. Measurements could be performed in 161 scans (27%) in 79 patients (75%) (**Table 1**). As an example, **Figure 3** shows all measurements.

Table 2 depicts the embryonic brain structure measurements per week GA with the corresponding mean value and SD value. We were able to measure the mesencephalon, diencephalon and telencephalon as early as 7^{+1} weeks' GA.

Ultrasound characteristics	**7 weeks' GA Mean (SD)**	**8 weeks' GA Mean (SD)**	**9 weeks' GA Mean (SD)**	**10 weeks' GA Mean (SD)**	**11 weeks' GA Mean (SD)**	**12 weeks' GA Mean (SD)**
CRL (mm)	12.25 (3.27)	18.42 (3.46)	25.93 (4.30)	36.17 (5.90)	48.46 (7.13)	61.54 (7.49)
N	15/95	36/97	34/100	34/104	25/103	17/97
DTL (mm)	0.85 (0.19)	1.21 (0.33)	1.69 (0.28)	2.34 (0.42)	3.24 (0.48)	3.90 (0.57)
DTR (mm)	0.83 (0.18)	1.23 (0.33)	1.68 (0.26)	2.29 (0.39)	3.19 (0.45)	3.88 (0.57)
DTD (mm)	2.85 (0.39)	3.41 (0.76)	4.37 (0.50)	5.64 (0.75)	7.20 (0.93)	8.61 (1.08)
MTL (mm)	0.74 (0.19)	0.92 (0.22)	1.24 (0.26)	1.66 (0.31)	2.07 (0.20)	2.40 (0.29)
MTR (mm)	0.77 (0.14)	0.95 (0.21)	1.23 (0.29)	1.71 (0.29)	2.08 (0.23)	2.34 (0.26)
MTD (mm)	2.52 (0.47)	3.21 (0.60)	4.08 (0.52)	5.16 (0.56)	6.00 (0.39)	6.42 (0.37)
TTL (mm)	0.58 (0.12)	0.76 (0.22)	1.15 (0.26)	1.38 (0.21)	1.76 (0.32)	1.88 (0.31)
TTR (mm)	0.58 (0.07)	0.80 (0.22)	1.17 (0.27)	1.49 (0.28)	1.82 (0.29)	2.05 (0.35)

Table 2: mean estimations with the corresponding SD and number (N) of images per complete gestational week
CRL, crown-rump length; DTL, diencephalon thickness left; DTR, diencephalon thickness right; DTD, diencephalon total diameter; MTL, mesencephalon thickness left; MTR, mesencephalon thickness right; MTD, mesencephalon total diameter; TTL, telencephalon thickness left; TTR, telencephalon thickness right; SD, standard deviation

The mean (percentage) difference, the limits of agreement and the ICC values for the intra- and inter-observer reproducibility of the 3D measurements are displayed in **Table 3**. All ICC values were >0.98, representing very good reliability between the measurements. The Bland–Altman statistics showed good agreement between the measurements for all parameters except

Agreement	Mean difference (mm)	95% CI mean difference (mm)	95% limits of agreement (mm)	Mean difference (%)	95% limits of agreement (%)	ICC	95% CI ICC
Intra-observer							
DTL	−0.01	−0.03 to 0.00	−0.09 to 0.07	−0.52	−6.48 to 5.45	0.999	0.999–1.000
DTR	−0.02	−0.06 to 0.01	−0.21 to 0.17	−0.72	−12.74 to 11.31	0.996	0.993–0.998
DTD	−0.02	−0.05 to 0.01	−0.17 to 0.13	0.34	−3.33 to 2.65	0.999	0.999–1.000
MTL	0.02	−0.01 to 0.05	−0.14 to 0.18	1.75	−9.90 to 13.41	0.993	0.986–0.997
MTR	0.00	−0.03 to 0.33	−0.18 to 0.18	−0.31	−11.23 to 10.61	0.991	0.982–0.996
MTD	−0.01	−0.05 to 0.03	−0.22 to 0.21	0.00	−4.45 to 4.46	0.997	0.995–0.999
TTL	−0.02	−0.06 to 0.01	−0.22 to 0.17	−1.82	−18.45 to 14.82	0.986	0.971–0.993
TTR	−0.01	−0.04 to 0.02	−0.19 to 0.17	0.29	−17.51 to 18.09	0.990	0.980–0.995
Inter-observer							
DTL	−0.01	−0.03 to 0.01	−0.12 to 0.11	−0.62	−7.46 to 6.22	0.999	0.998–0.999
DTR	−0.03	−0.06 to 0.00	−0.19 to 0.14	−0.95	−13.00 to 11.09	0.997	0.994–0.999
DTD	0.04	−0.00 to 0.08	−0.19 to 0.27	−0.74	−3.60 to 5.07	0.998	0.996–0.999
MTL	−0.03	−0.06 to 0.00	−0.20 to 0.14	−2.74	−18.39 to 12.91	0.992	0.982–0.996
MTR	0.00	−0.04 to 0.04	−0.21 to 0.21	−1.15	−18.50 to 16.20	0.988	0.974–0.994
MTD	0.05	−0.01 to 0.11	−0.27 to 0.37	1.66	−7.18 to 10.50	0.994	0.987–0.997
TTL	−0.05	−0.09 to −0.01	−0.26 to 0.16	−6.87	−31.39 to 17.64	0.980	0.950–0.991
TTR	0.03	−0.01 to 0.07	−0.20 to 0.26	0.45	−20.28 to 21.19	0.982	0.963–0.992

Table 3: mean difference with the corresponding CI, the limits of agreement and the ICCs with the corresponding 95% CI
DTL, diencephalon thickness left; DTR, diencephalon thickness right; DTD, diencephalon total diameter; MTL, mesencephalon thickness left; MTR, mesencephalon thickness right; MTD, mesencephalon total diameter; TTL, telencephalon thickness left; TTR, telencephalon thickness right; CI, confidence interval; ICC, intra-class correlation coefficient

the telencephalon thickness. Measurements of the total diameters of the diencephalon and mesencephalon showed better agreement compared with those of the individual left and right thicknesses.

There was no significant difference between the left and right thicknesses of the mesencephalon (mean difference = −0.02 mm, range −0.04–0.00 mm; P = 0.068). However, there was a small statistically significant difference between the left and right thicknesses of the diencephalon (mean difference = 0.02 mm, range 0.00–0.04 mm; P = 0.013) and between the left and right thicknesses of the telencephalon (mean difference = −0.07 mm, range −0.10 to −0.05 mm; P < 0.0001). Since we considered these differences too small to be clinically significant, we averaged left and right data to create the size charts of the embryonic brain structures.

The size charts of the embryonic brain structures are shown in **Figure 2**.

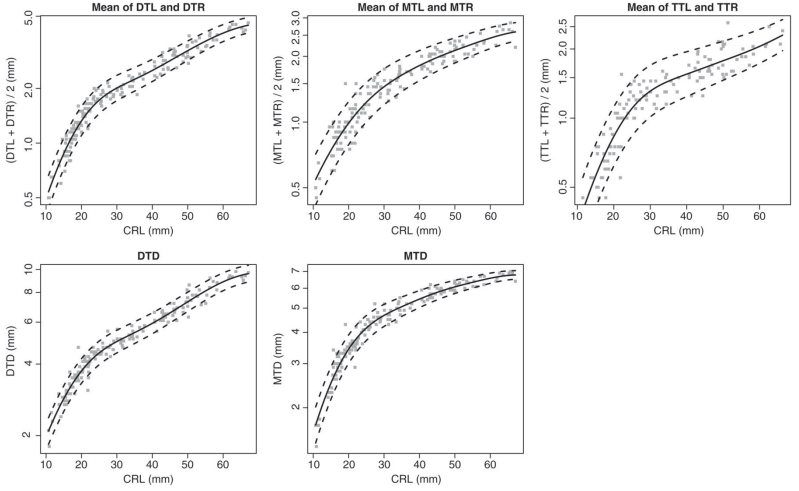

Figure 2: the embryonic brain structures against the CRL. The lines represent the p5, p50 and p95 reference lines. DTL, diencephalon thickness left; DTR, diencephalon thickness right; DTD, diencephalon total diameter; MTL, mesencephalon thickness left; MTR, mesencephalon thickness right; MTD, mesencephalon total diameter; TTL, telencephalon thickness left; TTR, telencephalon thickness right.

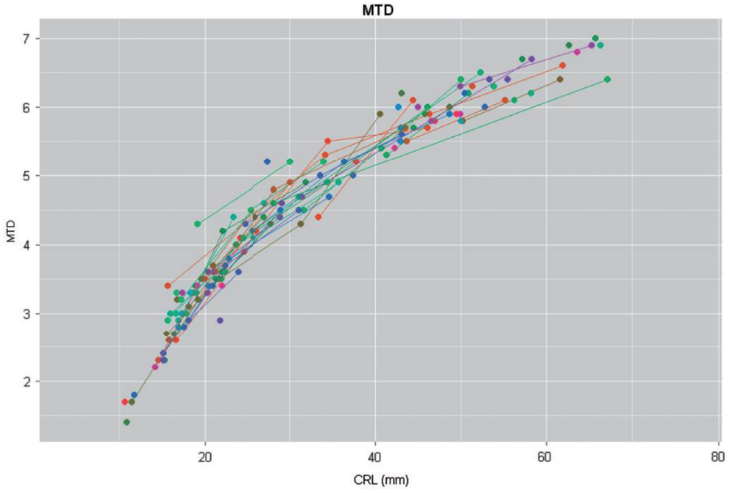

Figure 3: the raw longitudinal representation of all measurements of the mesencephalon total diameter (MTD) against the crown-rump length (CRL, with lines connecting pregnancies with multiple observations.

Discussion

This explorative study shows that the use of a high-frequency transvaginal transducer allows for accurate and reproducible measurements of embryonic brain structures on 3D data sets from 7 weeks' GA onwards, namely the diencephalon, mesencephalon and telencephalon, to create size charts.

A good reliability was found for intra-observer and inter-observer measurements of all brain parameters. However, measurements of the total diameters of the diencephalon and mesencephalon showed a better agreement compared with those of the individual left and right thicknesses. This may be due to a better visualisation of the outer borders compared with the inner borders of the diencephalon and mesencephalon. The wider limits of agreement found for the telencephalon thickness can be explained by the poor

demarcation of the borders of the telencephalon and the large variability in size with minimal adjustment of the scan. In addition, because of the low success rate of the measurements of the telencephalon (22%), the measurement errors reduce the precision and reliability of these measurements. We point out that our assessment of reproducibility is limited. It is based on the same stored ultrasound images, evaluated by different observers. For a full assessment, it would be necessary to collect and measure repeated (suitable) images of the same embryos. Such data are not available. In addition, in this study each volume required manual adjustment to obtain the right image for measurement, which implies that also image reading was part of the reproducibility that has been tested.

Blaas and Eik-Nes described human brain development in the first trimester of pregnancy.[1] 3D US reconstructions of the embryo and the embryonic brain (cavities) in particular have been available in the literature since the early 1990s.[7, 9, 10, 17] Due to improvements in ultrasound equipment and their increasingly widespread availability, the embryonic and foetal brain can be investigated in much larger populations. Measurements of developing embryonic brain structures allow us to create size charts, which may enable differentiation between anatomically normal and abnormal human brain development in early pregnancy.

One will not expect that measurements of the brain mantle are helpful in the diagnosis of all congenital malformations that occur in the embryonic period, such as holoprosencephaly and neural tube defects. In these pathological conditions, diagnosis is made by identification of gross anatomical derangements. However, in cases of ventriculomegaly, one could argue that measurements of the total diameters of the mesencephalon and diencephalon are more easily performed than measurements of the cavities due to better demarcation of the outer borders in comparison with the inner borders of the brain mantle. Our standardised cross sections of the embryonic brain allow reliable measurements of total mesencephalon and diencephalon diameters.

Several studies have been performed measuring embryonic brain cavities.[11, 13, 18] When subtracting the diameters of the walls from the total diameters, the widths of the brain cavities are obtained. Both the widths of the cavities of the diencephalon and the mesencephalon in this study show virtually identical values from 7 to 12 weeks compared with those measured by Blaas et al.[13]

Tanaka and Hata performed measurements of the walls of the brain vesicles, diencephalon, mesencephalon, metencephalon and telencephalon using 2D intrauterine sonography. We have measured slightly greater thicknesses of the diencephalon, mesencephalon and telencephalon, which may be explained by a somewhat different measurement method. In their study, 71 scans were used when compared with 161 scans in our study. The relatively lower feasibility can be explained by the use of a 20 MHz intrauterine transducer, a technique that cannot be implemented in daily practice. In comparison with the use of our transvaginal transducer, transducer movement is less limited, allowing a better visualisation of the embryonic structures. Other differences are that their patients were about to undergo therapeutic termination of pregnancy, foetal abnormalities could not be ruled out, and the measurements were performed one sided which suggests a less strict selection of scans.

In our study, we not only measured both right and left thicknesses of the diencephalon and mesencephalon but also measured the right and left thicknesses of the telencephalon. We found a slight asymmetry in the thicknesses of the diencephalon and the telencephalon. An explanation could be the 3D acquisition and measurement biases. Another explanation is that brain asymmetry (like asymmetry of the lateral ventricles in normal foetuses) is already present in the embryo as a normal physiological variation. For now, we pooled the data of the left and right thicknesses of the brain structures, because of the lack of clinical significance of these small differences. This reduced the measurement noise appreciably, increasing precision and validity of the size charts of the embryonic brain structures.

There are several explanations for the low percentage (27%) of scans suitable for analysis of these embryonic brain structures. Although high-frequency transvaginal transducers result in a better resolution and allow for more magnification, the quality of the scans declines rapidly with increasing depth. Movement artefacts due to embryonic or maternal movements were another important reason for exclusion of 3D volumes. Finally, the present study was embedded in a prospective cohort study. 3D US sweeps encompassing the whole embryo, to measure the embryonic volume for example, were obtained weekly without specific brain-targeted imaging; 3D US examinations dedicated to the embryonic brain (structures) would have undoubtedly leaded to a higher success rate. However, when accounting for the number of weekly measurements per pregnancy, the average percentage of successful measurements per number of scans per pregnancy was >33% for all measurements. The non-response analysis comparing the characteristics between the pregnancies that did and did not provide measurable scans did not show any significant differences. Therefore, selection bias is not very likely. Surprisingly, the embryonic brain structures of smaller embryos could be measured more often. Since neither the size of the embryo nor the characteristics of the pregnancies can explain the cause of data loss, motion artefacts or other reasons for low-quality images become more likely.

The average number of successive measurements is only 2. This implies that the current study contains both longitudinal and cross-sectional data, and is therefore a mixed study. Since in 41–52% of pregnancies only one measurement could be performed and we are not interested in confidence intervals in our size charts at this moment, we chose to carry out a cross-sectional analysis in which we described the trends and spread in the study population of this observational study. A limitation of this type of analysis is that we handled the data as being cross-sectional, although for a (small) fraction of the embryos multiple measurements were included. Hence, not all data points were independent and our charts should be interpreted carefully.

In all graphs we see a 'bump', being more prominent in the graphs of the diencephalon and telencephalon. This corresponds to a GA between 9 and 10 weeks and can be explained by a relatively increased growth in this period due to the transfer of histiotrophic to haemotrophic nutrition of the embryo.[19, 20] In our periconception cohort study, more research onto this phenomenon is being carried out.

In conclusion, it was feasible to create reliable size charts of human embryonic brain structures, even with the limited eligibility of scans. In high-quality images, the reliability of embryonic brain structure measurements is excellent. The size charts of human embryonic brain structures can be used to study normal and abnormal brain development in future. Also, the effects of periconceptional maternal exposures, such as folic acid supplement use and smoking on human embryonic brain development can be a topic of future research. Multivariate analyses will allow us to come to a better understanding of very early human brain development.

References

1. Blaas HG, Eik-Nes SH. Sonoembryology and early prenatal diagnosis of neural anomalies. Prenat Diagn. 2009;29(4):312-25.
2. Thompson BL, Levitt P, Stanwood GD. Prenatal exposure to drugs: effects on brain development and implications for policy and education. Nat Rev Neurosci. 2009;10(4):303-12.
3. Willford J, Day R, Aizenstein H, Day N. Caudate asymmetry: a neurobiological marker of moderate prenatal alcohol exposure in young adults. Neurotoxicol Teratol. 2010;32(6):589-94.
4. Fong KW, Toi A, Salem S, Hornberger LK, Chitayat D, Keating SJ, et al. Detection of fetal structural abnormalities with US during early pregnancy. Radiographics. 2004;24(1):157-74.
5. O'Rahilly R, Muller F. Significant features in the early prenatal development of the human brain. Ann Anat. 2008;190(2):105-18.
6. O'Rahilly R, Muller F. Developmental stages in human embryos: revised and new measurements. Cells Tissues Organs. 2010;192(2):73-84.
7. Timor-Tritsch IE, Monteagudo A. Transvaginal sonographic evaluation of the fetal central nervous system. Obstet Gynecol Clin North Am. 1991;18(4):713-48.
8. Timor-Tritsch IE, Monteagudo A, Warren WB. Transvaginal ultrasonographic definition of the central nervous system in the first and early second trimesters. Am J Obstet Gynecol. 1991;164(2):497-503.
9. Blaas HG, Eik-Nes SH, Berg S, Torp H. In-vivo three-dimensional ultrasound reconstructions of embryos and early fetuses. Lancet. 1998;352(9135):1182-6.
10. Berg S, Torp H, Blaas HG. Accuracy of in-vitro volume estimation of small structures using three-dimensional ultrasound. Ultrasound Med Biol. 2000;26(3):425-32.
11. Tanaka H, Senoh D, Yanagihara T, Hata T. Intrauterine sonographic measurement of embryonic brain vesicle. Hum Reprod. 2000;15(6):1407-12.
12. Tanaka H, Hata T. Intrauterine sonographic measurement of the embryonic brain mantle. Ultrasound Obstet Gynecol. 2009;34(1):47-51.
13. Blaas HG, Eik-Nes SH, Kiserud T, Hellevik LR. Early development of the forebrain and midbrain: a longitudinal ultrasound study from 7 to 12 weeks of gestation. Ultrasound Obstet Gynecol. 1994;4(3):183-92.

14. Blaas HG, Eik-Nes SH, Kiserud T, Berg S, Angelsen B, Olstad B. Three-dimensional imaging of the brain cavities in human embryos. Ultrasound Obstet Gynecol. 1995;5(4):228-32.

15. Bland JM, Altman DG. Applying the right statistics: analyses of measurement studies. Ultrasound Obstet Gynecol. 2003;22(1):85-93.

16. Rigby RA, Stasinopoulos DM. Generalized additive models for location, scale and shape. J Roy Stat Soc C-App. 2005;54:507-44.

17. Timor-Tritsch IE, Monteagudo A, Santos R. Three-dimensional inversion rendering in the first- and early second-trimester fetal brain: its use in holoprosencephaly. Ultrasound Obstet Gynecol. 2008;32(6):744-50.

18. Blaas HG, Eik-Nes SH, Kiserud T, Hellevik LR. Early development of the hindbrain: a longitudinal ultrasound study from 7 to 12 weeks of gestation. Ultrasound Obstet Gynecol. 1995;5(3):151-60.

19. Burton GJ, Hempstock J, Jauniaux E. Nutrition of the human fetus during the first trimester—a review. Placenta. 2001;22 Suppl A:S70-7.

20. van Uitert EM, Exalto N, Burton GJ, Willemsen SP, Koning AH, Eilers PH, et al. Human embryonic growth trajectories and associations with fetal growth and birthweight. Hum Reprod. 2013;28(7):1753-61.

CHAPTER 3

Evaluation of first trimester physiological midgut herniation using 3D ultrasound

Bogers H, Baken L, Cohen-Overbeek TE, Koning AHJ, Willemsen SP, Spek PJ van der, Exalto N, Steegers EAP

Fetal Diagn Ther. 2018 Aug 15:1-7 [Epub ahead of print]

Abstract

Introduction: The aim of the study was to investigate the development of the midgut herniation in vivo using 3D ultrasonographic volume- and distance measurements and to create reference data for the physiological midgut herniation in ongoing pregnancies in a tertiary hospital population.

Material and Methods: Transvaginal 3D ultrasound volumes of 112 women, seen weekly during first trimester of pregnancy, were obtained and subsequently analysed in a virtual reality environment. The width of the umbilical cord insertion, the maximum diameter of the umbilical cord and the volume of the midgut herniation were measured from 6 until 13 weeks gestational age (GA).

Results: All parameters had a positive relation with the GA, crown-rump length and abdominal circumference. In approximately 1 in 10 volumes no midgut herniation could be observed at 9 and 10 weeks GA. In 5.0% of the foetuses at 12 weeks GA the presence of a midgut herniation could still be visualised.

Discussion: Reference charts for several different dimensions of the physiological midgut herniation were created. In future, our data might be used as a reference in the first trimester for comparison in case of a suspected pathological omphalocoele.

Introduction

A congenital omphalocoele, defined as the presence of visceral contents in the umbilical cord, can be detected from 12 weeks GA onwards.[1-3] Before 12 weeks there is a temporary physiological midgut herniation. There is an increasing interest in detecting structural abnormalities in the first trimester of pregnancy.[4, 5] Although a large congenital omphalocoele can be detected before 12 weeks GA,[6] false positive diagnosis may be as high as 32% during the first trimester[7] and small omphalocoeles may disappear later in pregnancy.[8] Kagan et al. even described a spontaneous resolution at 20 weeks in 92.5% of first trimester diagnosed omphalocoeles in euploid foetuses.[9] Three-dimensional (3D) imaging may be helpful in confirming the diagnosis and counselling patients.[10]

Between 7 and 12 weeks gestational age (GA) the midgut herniates into the umbilical cord. This midgut herniation (sometimes called physiological omphalocoele) is caused by a relatively rapid growth of the midgut, accompanied by a 270^0 anticlockwise midgut rotation in the abdominal cavity. Return into the body is caused by a rapid growth of the body or a decrease in the length of the mesentery. Failure may result in a (pathological) congenital omphalocoele. Since this does not explain the possible herniation of other organs like the liver, Achiron et al. differentiated between an omphalocoele caused by a failure to form the primitive umbilical ring and a failed return of the midgut from the umbilical cord.[11] This would also explain the spontaneous resolution of small omphalocoeles. Herniation was already observed in an in vitro study at Carnegie stage 16 (about 7 weeks and 2 days GA) and at 11 weeks GA the herniated intestine was still present in half of the cases.[2]

Technical developments in three-dimensional (3D) ultrasound techniques, including 3D virtual reality (3D VR) have resulted in progress in visualisation of the foetus and foetal volume measurements as well.[12] The aim of this study was to investigate the presence and size of the midgut herniation in a normally developing foetus using 3D ultrasonographic volume- and distance measurements and to develop reference charts for the dimensions of the midgut herniation during organogenesis.

Material and Methods

Study population and samples

This study has been conducted in a periconception cohort study at a university hospital for which women were enrolled for first trimester longitudinal 3D ultrasound measurements to evaluate foetal growth and development using new imaging techniques. Pregnant women who participated were enrolled between 6 and 8 weeks GA via the outpatient clinic of the department of Obstetrics and Gynaecology and local midwifery practices. All women received once weekly 3D ultrasound scans between 6^{+0} and 12^{+6} weeks GA. Only women less than eight weeks pregnant with a singleton pregnancy entered the study for further analysis.

We selected from the cohort 141 women who were enrolled in 2009 and from whom at least one volume was obtained. Two pregnancies complicated with trisomy 21 and three with congenital anomalies were excluded. Three multiple pregnancies, three drop outs, 16 miscarriages and two cases with an intrauterine foetal demise had to be excluded as well, leaving 112 inclusions for analysis (**Figure 1**).

Since an exomphalos is a common feature of Edwards syndrome, after finishing the study we also looked at available ultrasound volumes of trisomy 18 cases that have been described before.[13]

Ethical approval

All participants signed a written informed consent form and the local medical and ethical review committee approved the study protocol (METC 232.394/2003/177, METC 323.395/2003/178, MEC 2004–227).

Pregnancy dating

The GA was calculated according to the first day of the last menstrual period (LMP) in case of a regular menstrual cycle of 28 days and adjusted for a longer or shorter cycle.[14] In case of a discrepancy in GA of more than seven days between crown rump length (CRL) and the last menstrual period

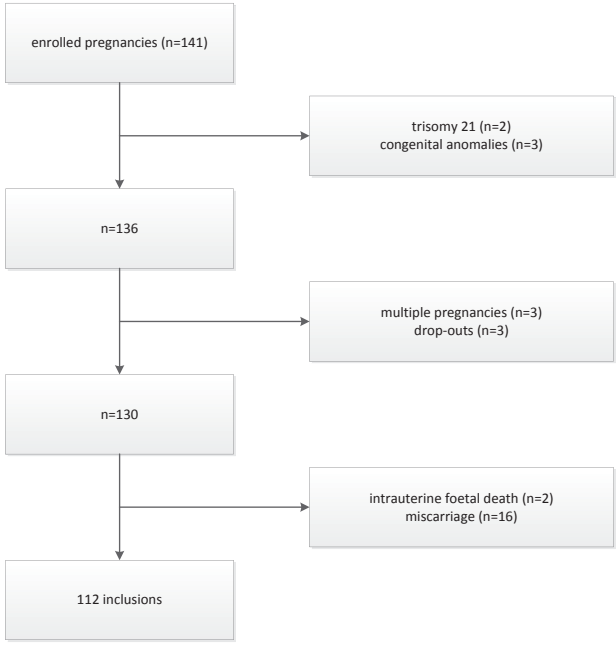

Figure 1: flowchart illustrating inclusions and exclusions of the study population

(LMP), or an unknown LMP, the GA was calculated by using CRL according to Robinson[15] at the end of the first trimester using the latest available measurement. In case of assisted reproductive technology, GA was determined by the date of oocyte retrieval plus 14 days in pregnancies conceived via in vitro fertilisation with or without intracytoplasmic sperm injection (IVF/ICSI) procedures, from the LMP or insemination date plus 14 days in pregnancies conceived through intrauterine insemination, and from the day of embryo transfer plus 17 or 18 days in pregnancies originating from the transfer of cryopreserved embryos, depending on the number of days between oocyte retrieval and cryopreservation of the embryo.

Material

The sonographic volumes were acquired using a Voluson E8 ultrasound machine (GE Medical Systems, Zipf, Austria) and obtained with a transvaginal scan (GE-probe RIC-6-12-D [4.5–11.9 MHz]). With regard to the safety aspects of first trimester ultrasound the thermal index (TI) and mechanical index (MI) were kept below 1.0, the examiners were qualified and experienced, and the as-low-as-reasonable-practicable (ALARP) principle was respected: the duration of the examination did not exceed 30 minutes, and 3D images were stored for offline evaluation in order to reduce the exposure to ultrasound as much as possible.[16] The 3D volumes were converted to a Cartesian format and visualised in the BARCO I-Space (Barco N.V., Kortrijk, Belgium). This is a four-walled CAVE™-like (Cave Automatic Virtual Environment) virtual reality system.[12] The V-Scope volume rendering application is used to create a 'hologram' of the ultrasound volume that is being investigated, floating in space in front of the observer.[17] For our study the 3D volumes were resized (enlarged), rotated and cropped when necessary and grey-scale and opacity values were adjusted for optimal image quality.

Measurements

Using the 3D VR wireless joystick, we first determined whether we could observe the midgut to protrude in the umbilical cord. If so, just above the level of the insertion we measured in a midsagittal plane the anteroposterior diameter of the abdomen (APD), perpendicular to the spine. In an axial plane we measured perpendicular to this diameter the transverse diameter of the abdomen (TD) in order to calculate the abdominal circumference (AC): $AC = \pi[0.75(APD+TD)-\sqrt{(APD*TD)/4}]$. Then, we measured the maximum width of the midgut herniation and the width of the cord insertion in an axial plane as well (**Figure 2**). After these measurements we erased all voxels surrounding the midgut herniation. The volume of this free floating midgut herniation could be determined semi-automatically by placing a seed point in the midgut herniation and using the region growing segmentation algorithm implemented in the V-Scope application (**Figure 2**).

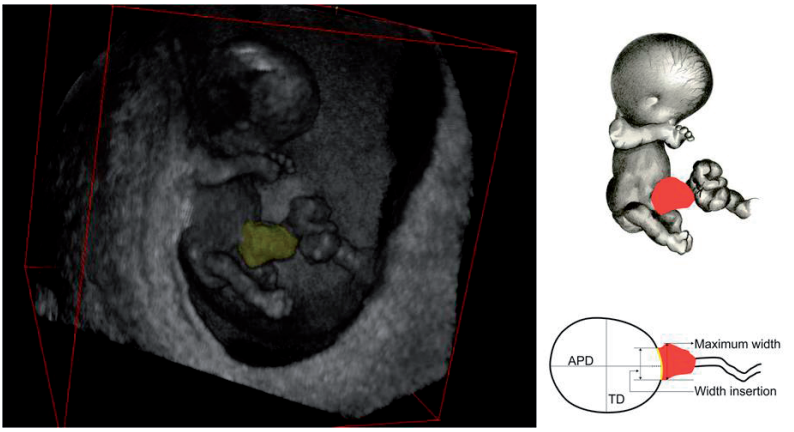

Figure 2: semi-automatic volume measurement of the free floating midgut herniation in the BARCO I-Space (left) and schematic representation of measurements (right); APD: anteroposterior diameter of the abdomen, TD: transverse diameter of the abdomen

All measurements were performed offline. Measurements of 31 foetuses were randomly repeated once by the same examiner (LB) and once by another examiner (HB) to study the reproducibility by determining the intraobserver and interobserver variability.

Statistical analysis

We created references curves for the maximum width of the midgut herniation and the width of the cord insertion, and the volume of the midgut herniation. These parameters were plottedagainst the GA, AC and CRL. This was done using the GAMLSS (generalised additive models for location scale and shape) methodology using the eponymous R-package.[18] It is assumed that the responses follow a (truncated) normal distribution after applying a Box-Cox transformation. The parameters of this distribution are modelled as a spline function of the independent variable.

The intraobserver and interobserver variability was depicted with Bland Altman plots indicating the bias (the systematic of mean difference between two measurements, with 95%CI) and the upper and lower limits of agreement (LOAs, with 95%CIs). The Repeatability Coefficient and Intraclass correlation coefficients (ICCs, two way mixed, single measures, absolute agreement) of intraobserver and interobserver measurements were added.

Results

From the 112 pregnancies 699 volumes were obtained for evaluation (mean: 6.24, median: 6, range: 4-8 volumes per patient). Patient characteristics are presented in **Table 1**. Of these 699 volumes, a midgut herniation was

Characteristic	**Median (range) or percentage**
Singleton pregnancies (n=112)	
Maternal age (years)	32.9 (18.9-42.7)
Gravidity	2 (1-10)
Parity	
0	62.5%
1	27.7%
≥ 2	9.8%
Miscarriages ≥ 2	25.9%
Conception mode	
Natural	70.5%
IVF or IVF/ICSI	27.7%
Intrauterine insemination	1.8%
Gestational diabetes	5.4%
Hypertensive disorders	8.9%
Small-for-gestational age	3.6%
Newborns (n=112)	
Female	52.7%
Birth weight (grams)	3390 (450-4700)
GA at delivery (weeks)	39^{+4} (26^{+4} – 42^{+0})

Table 1: general characteristics of the study population

present in 305 volumes. Measurements could be performed in 181 out of 305 volumes (59.3%). Besides one foetus (with very low quality of all the acquired volumes), in all foetuses at some moment a herniation was seen. In our data set in approximately 1 in 10 ultrasound volumes no midgut herniation could be observed at 9 and 10 weeks GA. The earliest and latest GA we were able to measure a midgut herniation was 7 weeks and 3 days and 12 weeks and 1 day respectively (**Table 2**). Reference values of the width of the cord insertion, the maximum width and the volume of the herniation are provided in **Table 3**, **4** and **5** respectively. In **Figure 3** the width of the cord insertion is plotted against the GA, CRL and AC. Although there is a positive linear relation with all parameters, this effect is most prominent at an early GA and smaller CRL and AC. The same results were obtained regarding the maximum width and the volume of the midgut herniation - plotted against the GA, CRL and AC.

We found six cases of trisomy 18 between 12 weeks and 0 days and 13 weeks and 1 day, more or less immediately following the time period of study of our current manuscript (7 weeks and 3 days - 12 weeks and 1 days). Volume measurements in these six cases were much larger (median:

Week	Number of volumes	Midgut herniation absent	%	Midgut herniation present	%	Success rate	%
6	65	65	100.0	0	0.0	-	-
7	101	91	90.1	10	9.9	3/10	30.0
8	106	47	44.3	59	55.7	29/59	49.2
9	107	10	9.3	97	90.7	62/97	63.9
10	110	12	10.9	98	89.1	67/98	68.4
11	109	73	67.0	36	33.0	17/36	47.2
12	101	96	95.0	5	5.0	3/5	60.0
Total	699	394	56.4	305	43.6	181/305	59.3

Table 2: absolute and relative numbers of absent and present midgut herniations and success percentages of measurements (measurement/number of volumes with discernible midgut herniation; %) by gestational age (expressed in complete weeks)

GA	p5	p50	p95	number of volumes measured
8^{+0}	1.67	2.21	2.87	29
9^{+0}	2.03	2.70	3.52	62
10^{+0}	2.42	3.26	4.27	67
11^{+0}	2.46	3.33	4.39	17
12^{+0}	2.45	3.35	4.44	3

Table 3: reference values of the width of the cord insertion (mm); GA: gestational age

GA	p5	p50	p95	number of volumes measured
8^{+0}	2.22	3.23	4.19	29
9^{+0}	2.89	4.04	5.14	62
10^{+0}	3.55	4.79	5.97	67
11^{+0}	3.84	5.01	6.14	17
12^{+0}	3.89	4.94	5.96	3

Table 4: reference values of the maximum width of the midgut herniation (mm); GA: gestational age

GA	p5	p50	p95	number of volumes measured
8^{+0}	17.76	27.16	37.95	29
9^{+0}	21.07	44.19	73.07	62
10^{+0}	30.68	67.76	114.65	67
11^{+0}	42.51	82.02	130.34	17
12^{+0}	75.99	90.01	104.89	3

Table 5: reference values of the volume of the midgut herniation (mm^3); GA: gestational age

182.6 mm^3; range: 71.4 - 995.6 mm^3) as compared to our reference data (median: 59.0 mm^3, range: 13.9 - 146.1 mm^3).

The mean differences, the 95% limits of agreement and the intraclass correlation coefficients (ICC) of intra- and interobserver variability are shown in **Table 6**. ICC's were all >0.9 indicating excellent reproducibility.

	Mean difference (95%CI)		Lower LOA (95%CI)		Upper LOA (95%CI)		Repeatibility Coefficient		ICC	
	intra	inter	intra	inter	intra	inter	intra	inter	intra	inter
width of insertion	0.037 (-0.56 ; 0.130)	0.008 (-0.081 ; 0.097)	-0.469 (-0.630 ; -0.308)	-0.478 (-0.633 ; -0.324)	0.543 (0.382 ; 0.703)	0.494 (0.340 ; 0.649)	0.506	0.486	0.920	0.917
maximum width	0.020 (-0.075 ; 0.115)	0.037 (-0.043 ; 0.118)	-0.500 (-0.665 ; -0.335)	-0.401 (-0.540 ; -0.262)	0.540 (0.375 ; 0.705)	0.475 (0.336 ; 0.615)	0.520	0.438	0.951	0.962
volume	0.703 (-0.056 ; 1.463)	0.285 (-0.456 ; 1.025)	-3.438 (-4.753 ; -2.122)	-3.753 (-5.035 ; -2.470)	4.844 (3.529 ; 6.159)	4.322 (3.040 ; 5.605)	4.141	4.038	0.997	0.997

Table 6: intra- and inter observer variability; LOA: limits of agreement, ICC: intraclass correlation coefficient

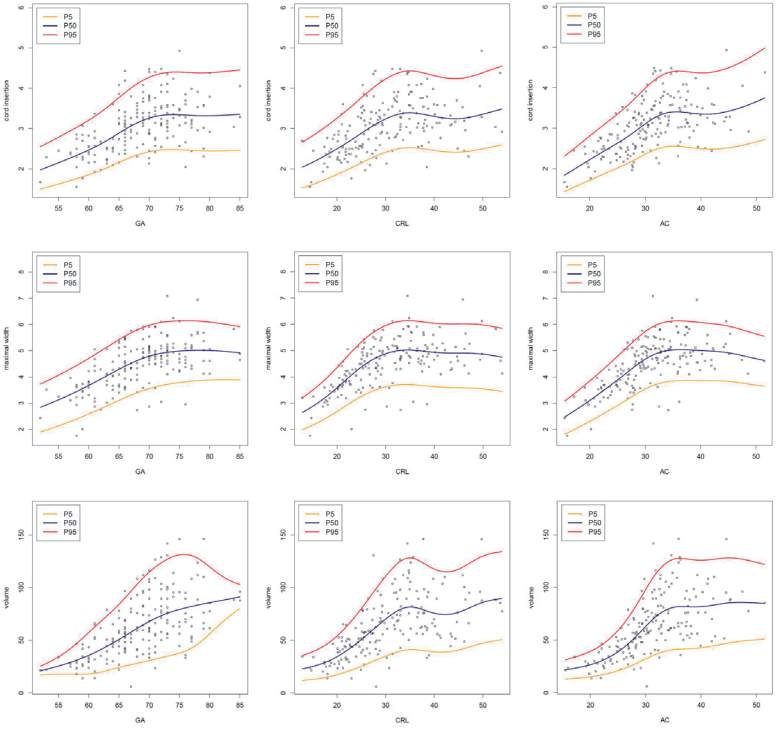

Figure 3: the width of the cord insertion (mm), the maximum width of the midgut herniation (mm) and the volume of the midgut herniation (mm^3) as a function of respectively gestational age (GA; days), crown-rump length (CRL; mm) and the abdominal circumference (AC; mm)

Discussion

We investigated the early foetal development of the umbilical cord insertion by means of 3D ultrasound. The midgut herniation could be measured reliably and reference curves were constructed for the volume and maximum width of the midgut herniation and the width of the umbilical cord insertion. Although we are not the first to investigate the midgut herniation by means

of ultrasound, all these studies had been performed in relatively few foetuses. Furthermore, most of these were done using 2D sonography.[1, 3, 6, 19]

In 1987 Schmidt et al. studied fourteen women weekly between 7 and 12 weeks GA.[1] The mean herniated mass was larger at 8 weeks GA (or 17-20 mm CRL) than at 9 weeks (or 23-26 CRL), which appears to be in contrast with our findings (**Figure 3**). The authors, however, found a noticeable variation in size of the mass at the same GA.

Blaas et al. investigated the development of several structures including the midgut herniation.[3] 29 women were seen five times from 7 to 12 weeks GA to measure - among others - the thickness of the umbilical cord at the insertion and its thickness in a free loop. At 7 weeks GA a thickening of the cord containing a slight echogenic area was seen, progressing to a large hyperechogenic mass during 9 and 10 weeks GA. The thickness of the umbilical cord at the insertion appeared to be increased between 8 and 11 weeks GA compared with the thickness in a free loop. From 10 weeks and 4 days the gut retracted and from 11 weeks and 5 days in none of the foetuses any herniation could be seen. In contrast, we observed at 12 weeks GA still a midgut herniation in a small minority of foetuses.

Bowerman investigated in 48 foetuses the midgut herniation.[19] From 11 weeks and 2 days GA no herniated midgut could be observed. In all cases but one scanning was performed transabdominally. The significant gap between his and our findings might be caused by the fact that we used high-resolution transvaginal instead of transabdominal ultrasound, most likely resulting in higher image quality.

The circumference of the midgut herniation was investigated weekly in 18 women by Van Zalen-Sprock et al.[6] between 7 and 12 weeks GA. The circumference of the midgut herniation appeared to be greatest at 10 weeks GA, with a maximum 24.5 mm, measured at the level of the insertion. Herniation could be observed in all foetuses at 10 weeks GA and in none of these at 12 weeks GA which is in contrast with our findings (98% and

5% respectively). This may be due to a relatively small number of cases in comparison to the present study. The different findings in the present study may be due to a much larger number of cases (18 vs 110 and 101).

3D evaluation of the midgut herniation has been investigated previously without performing measurements. Yonemoto et al. and Hata et al. compared in 5-11 weeks GA and 8-13 weeks GA respectively the visualisation rate of - among others - the midgut herniation. They showed 3D examination to be non-inferior to 2D examination, although this was not scientifically tested.[20, 21] Soffers et al. who investigated the rotation of the midgut in histological specimens used another novel 3D visualisation technique.[22] They used a technique in which serial sections of historical collections of embryos and foetuses were digitised using a scanning microscope. Subsequently these images were converted and aligned to create a 3D reconstruction. The several loops of the midgut appear to develop in a hierarchal manner and move independently of each other, facilitating phased return into the abdominal cavity. The authors state that the width of the hernia neck does not appear to determine the time window for intestinal return, which is supported by our finding that the width of the insertion does not increase after 10 weeks GA (**Figure 3**).

To our best knowledge, we are the first to perform volume measurements of the herniation. Another strong point of our study is the number of volumes that could be analysed, although this was somewhat limited by the success rate of the measurements. This could be due to the fact that in our study only non-targeted 3D sweeps of the entire foetus were stored. Movement artefacts of the foetus could have impeded accurate visualisation. Furthermore, the parameters were measured offline on stored data. All these aspects contributed to the suboptimal success rate.

In 5 out of 101 (5.0%) foetuses a midgut herniation could be observed at 12 weeks GA. Unfortunately we have only data available until 13 weeks GA. Further research in this period of gestation is necessary. The steeply decreasing number of foetuses with a midgut herniation from 11 weeks GA and the data from the literature however suggest a rapid disappearance after 12

weeks GA. In the careful postnatal follow up of our study group no congenital omphalocoeles have been reported. The larger measurements in the trisomy 18 cases at least supports the hypothesis that volume measurements may become a valuable diagnostic tool in diagnosing pathological omphalocoeles at the end of the first trimester. One should remain cautious however as spontaneous resolution of omphalocoeles have been described and a pathological omphalocoele during this period can easily be mistaken for a physiological midgut herniation. Since in only 5% of the foetuses at 12 weeks GA a midgut herniation was observed and the latest GA we could measure a herniation was 12 weeks and 1 day, we advise to repeat the examination when a herniation is observed at 12 weeks GA for this may be a pathological finding.

The proposed volume measurement technique cannot be done on conventional ultrasound machines with a 2D display, limiting its applicability. However, specialised 3D software is available to perform volume measurements on ultrasound machines or desktop computers. Also a user friendly 3D VR desktop system has been developed for routine use of diagnostic 3D VR ultrasound in an outpatient clinic, allowing precise length, volume and angle measurements.[23] By means of this system the volume measurements can easily be performed.

Conclusion

We created reference data for the midgut herniation in ongoing pregnancies. Our data may be used in future for studies on aetiology of abdominal wall defects and for comparison in foetuses in which at the first trimester ultrasound scan a congenital, pathological omphalocoele is suspected. Since in only 5% of the foetuses at 12 weeks GA a midgut herniation was observed and the latest GA we could measure a herniation was 12 weeks and 1 day, we advise to repeat the examination when a herniation is observed at 12 weeks GA for this may be a pathological finding.

Acknowledgements

We would like to thank Mr Hans Kneefel for helping creating **Figure 2**.

References

1. Schmidt W, Yarkoni S, Crelin ES, Hobbins JC. Sonographic visualization of physiologic anterior abdominal wall hernia in the first trimester. Obstet Gynecol. 1987;69(6):911-5.
2. Kim WK, Kim H, Ahn DH, Kim MH, Park HW. Timetable for intestinal rotation in staged human embryos and fetuses. Birth Defects Res A Clin Mol Teratol. 2003; 67(11):941-5.
3. Blaas HG, Eik-Nes SH, Kiserud T, Hellevik LR. Early development of the abdominal wall, stomach and heart from 7 to 12 weeks of gestation: a longitudinal ultrasound study. Ultrasound Obstet Gynecol. 1995;6(4):240-9.
4. Syngelaki A, Chelemen T, Dagklis T, Allan L, Nicolaides KH. Challenges in the diagnosis of fetal non-chromosomal abnormalities at 11-13 weeks. Prenat Diagn. 2011;31(1):90-102.
5. Chaoui R, Nicolaides KH. Detecting open spina bifida at the 11-13-week scan by assessing intracranial translucency and the posterior brain region: mid-sagittal or axial plane? Ultrasound Obstet Gynecol. 2011;38(6):609-12.
6. van Zalen-Sprock RM, Vugt JM, van Geijn HP. First-trimester sonography of physiological midgut herniation and early diagnosis of omphalocele. Prenat Diagn. 1997;17(6):511-8.
7. Lakasing L, Cicero S, Davenport M, Patel S, Nicolaides KH. Current outcome of antenatally diagnosed exomphalos: an 11 year review. J Pediatr Surg. 2006; 41(8):1403-6.
8. Blazer S, Zimmer EZ, Gover A, Bronshtein M. Fetal omphalocele detected early in pregnancy: associated anomalies and outcomes. Radiology. 2004;232(1): 191-5.
9. Kagan KO, Staboulidou I, Syngelaki A, Cruz J, Nicolaides KH. The 11-13-week scan: diagnosis and outcome of holoprosencephaly, exomphalos and megacystis. Ultrasound Obstet Gynecol. 2010;36(1):10-4.
10. Anandakumar C, Nuruddin Badruddin M, Chua TM, Wong YC, Chia D. First-trimester prenatal diagnosis of omphalocele using three-dimensional ultrasonography. Ultrasound Obstet Gynecol. 2002;20(6):635-6.
11. Achiron R, Soriano D, Lipitz S, Mashiach S, Goldman B, Seidman DS. Fetal midgut herniation into the umbilical cord: improved definition of ventral abdominal anomaly with the use of transvaginal sonography. Ultrasound Obstet Gynecol. 1995;6(4):256-60.

12. Rousian M, Hop WC, Koning AH, van der Spek PJ, Exalto N, Steegers EA. First trimester brain ventricle fluid and embryonic volumes measured by three-dimensional ultrasound with the use of I-Space virtual reality. Hum Reprod. 2013;28(5):1181-9.

13. Baken L, Benoit B, Koning AH, Willemsen SP, van der Spek PJ, Steegers-Theunissen RP, et al. First-trimester hand measurements in euploid and aneuploid human fetuses using virtual reality. Prenat Diagn. 2014;34(10):961-9.

14. Steegers-Theunissen RP, Verheijden-Paulissen JJ, van Uitert EM, Wildhagen MF, Exalto N, Koning AH, et al. Cohort Profile: The Rotterdam Periconceptional Cohort (Predict Study). Int J Epidemiol. 2016;45(2):374-81.

15. Robinson HP, Fleming JE. A critical evaluation of sonar "crown-rump length" measurements. Br J Obstet Gynaecol. 1975;82(9):702-10.

16. Knez J, Day A, Jurkovic D. Ultrasound imaging in the management of bleeding and pain in early pregnancy. Best Pract Res Clin Obstet Gynaecol. 2014;28(5): 621-36.

17. Koning AH, Rousian M, Verwoerd-Dikkeboom CM, Goedknegt L, Steegers EA, van der Spek PJ. V-scope: design and implementation of an immersive and desktop virtual reality volume visualization system. Stud Health Technol Inform. 2009;142:136-8.

18. Stasinopoulos DM, Rigby RA. Generalized additive models for location scale and shape (GAMLSS) in R. J Stat Softw. 2007;23(7).

19. Bowerman RA. Sonography of fetal midgut herniation: normal size criteria and correlation with crown-rump length. J Ultrasound Med. 1993;12(5):251-4.

20. Yonemoto H, Yoshida K, Kinoshita K, Takeuchi H. Embryological evaluation of surface features of human embryos and early fetuses by 3-D ultrasound. J Obstet Gynaecol Res. 2002;28(4):211-6.

21. Hata T, Aoki S, Manabe A, Hata K, Miyazaki K. Three-dimensional ultrasonography in the first trimester of human pregnancy. Hum Reprod. 1997;12(8): 1800-4.

22. Soffers JH, Hikspoors JP, Mekonen HK, Koehler SE, Lamers WH. The growth pattern of the human intestine and its mesentery. BMC Dev Biol. 2015;15:31.

23. Baken L, van Gruting IM, Steegers EA, van der Spek PJ, Exalto N, Koning AH. Design and validation of a 3D virtual reality desktop system for sonographic length and volume measurements in early pregnancy evaluation. J Clin Ultrasound. 2015;43(3):164-70.

CHAPTER 4

First trimester physiological development of the foetal foot position using three-dimensional ultrasound in virtual reality (3D VR)

Bogers H, Rifouna MS, Cohen-Overbeek TE, Koning AHJ, Willemsen SP, Spek PJ van der, Steegers-Theunissen RPM, Exalto N, Steegers EAP

Submitted

Abstract

Aim: In anatomic studies of the embryo it has been established that during development of the lower limb, several changes in foot position can be observed defined as a temporary 'physiological clubfoot'. The aim of this study was to develop and test a measurement tool for objective documentation of the first trimester foot position in vivo and to construct reference data for clinical use.

Methods: We developed a virtual orthopaedic protractor for measuring foot positioning using three-dimensional virtual reality visualisation. Three-dimensional ultrasound volumes of 112 pregnancies of women examined during the first trimester were studied in a BARCO I-Space. The frontal angle (plantar flexion) and the lateral angle (adduction) between the leg and foot were measured from 8 until 13 weeks gestational age.

Results: We observed that the frontal angle steadily decreases, whereas the lateral angle first increases, resulting in transient physiological clubfeet position at 10-11 weeks gestation, followed by a decrease to a normal foot position.

Conclusions: A transient clubfoot position is present during the normal development of the lower limbs and it has been measured in vivo for the first time. This study emphasises that a diagnosis of congenital clubfoot should not be made in the first trimester of pregnancy.

Introduction

There is an increasing interest in the detection of structural abnormalities in the first trimester of pregnancy.[1, 2] First trimester screening and technical improvement of ultrasound equipment have contributed to this shift of interest from the second trimester towards the first trimester of pregnancy. Detailed knowledge on sonographic appearance of normal first trimester development is essential, not only for early diagnosis of congenital anomalies but for the establishment of embryonic health.[3]

An idiopathic congenital clubfoot is one of the most common observed congenital anomalies with a reported incidence of 1 in 1000 live births.[4] Congenital clubfoot, or talipes equinovarus, is described as a fixation of the foot in adduction, in supination and in varus, with a medial rotation in relation to the talus of the calcaneus, navicular and cuboid bones, which are held in adduction and inversion by the ligaments and tendons.[5] Congenital clubfeet may be isolated but in approximately half of the cases they are associated with other anomalies in which case the prognosis is usually poor, e.g., neurological disorders (spina bifida), and chromosomal abnormalities and genetic factors.[6-8] In addition, congenital clubfoot is also associated with a relative lack of space in utero (e.g., twin pregnancy, oligohydramnios, early amniocentesis),[6] which was already presumed by Hippocrates in Ancient Greece.[9]

In anatomical studies of the embryo it was established that during development of the lower limb, several changes in foot position can be recognised, temporarily leading to a 'physiological clubfoot'.[10] Although different developmental pathways have been proposed, in all embryos a decrease in the angle of the foot with the frontal side of the leg (plantar flexion), and at first an increase followed by a decrease in the angle of the foot with the lateral side of the leg (adduction) is observed.

As the diagnosis of a congenital clubfoot is based on the subjective assessment of the ultrasound images there is, especially at the end of the first

trimester, a need for a measurement tool for objective documentation of the foot position. Recent developments in three-dimensional (3D) sonographic imaging techniques have resulted in remarkable progress in the visualisation of the developing foetus. Moreover, by using virtual reality (VR), e.g., the BARCO I-Space (Barco N.V., Kortrijk, Belgium), it is possible to immerse the viewer in a computer generated 3D environment, allowing him to perceive depth and to interact with volume-rendered (ultrasound) data in a more natural and intuitive manner than is possible with 3D views displayed on a two-dimensional (2D) screen.[11] This technique has provided new insights into normal as well as abnormal foetal growth and development.[11-13]

We developed a method for measuring the position of the foot by using a virtual orthopaedic protractor in VR, as the third dimension is necessary and essential for defining parallelism of two straight lines. This innovative foot positioning tool was tested for practical use in the first trimester, including reproducibility of measurements and developing reference curves for scientific and diagnostic purposes.

The aim of this study was to develop and evaluate a 3D VR measurement tool for objective documentation of first trimester foot position in vivo using VR and to construct reference data for foot position in ongoing pregnancies.

Methods

Study population and sample

This study has been conducted in a periconception cohort study at a university hospital for which women were enrolled for first trimester longitudinal 3D ultrasound measurements to evaluate foetal growth and development using 3D ultrasound and VR. Pregnant women who participated were enrolled via the outpatient clinic of the department of Obstetrics and Gynaecology and local midwifery practices. All women received weekly 3D ultrasound scans between 6+0 and 12+6 weeks GA. Only women less than eight weeks pregnant with a singleton pregnancy entered the study for further

analysis. All participants signed a written informed consent form and the local medical and ethical review committee approved the study protocol (MEC 2004-227 – 10 December 2009, combining: METC 232.394/2003/177, METC 323.395/2003/178, MEC 2004–227).

We selected from the cohort 141 women who were enrolled in 2009 and from whom at least one ultrasound volume was obtained and digitally stored in the so called "virtual embryo collection". Two pregnancies complicated with trisomy 21 and three with congenital anomalies were excluded. Three multiple pregnancies, three drop outs, 16 miscarriages and two cases with an intrauterine foetal demise had to be excluded as well, leaving 112 inclusions for analysis (**Figure 1**).

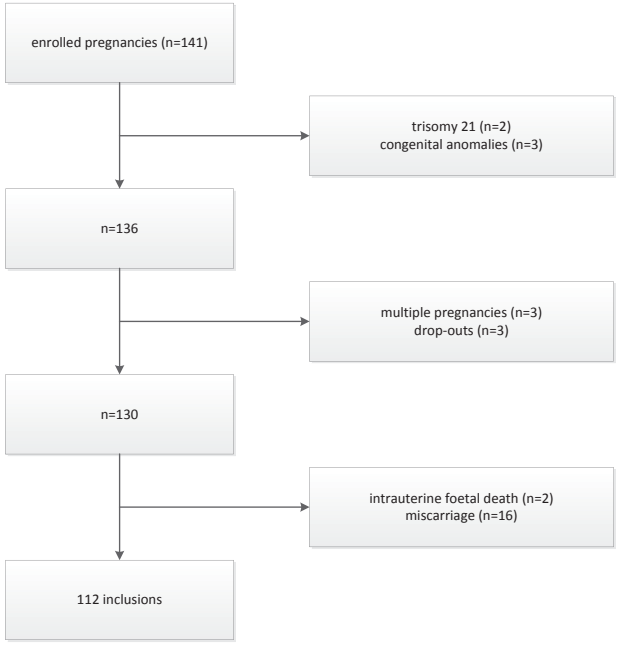

Figure 1: flowchart illustrating inclusions and exclusions of the study population

Pregnancy dating

The GA was calculated according to the first day of the last menstrual period (LMP) in case of a regular menstrual cycle of 28 days and adjusted for a longer or shorter cycle.[14] In case of a discrepancy in GA of more than seven days between crown rump length (CRL) and the last menstrual period (LMP), or an unknown LMP, the GA was calculated by using CRL at 12 weeks GA. In case of assisted reproductive technology, GA was determined by the date of oocyte retrieval plus 14 days in pregnancies conceived via in vitro fertilisation with or without intracytoplasmic sperm injection (IVF/ICSI) procedures, from the LMP or insemination date plus 14 days in pregnancies conceived through intrauterine insemination, and from the day of embryo transfer plus 17 or 18 days in pregnancies originating from the transfer of cryopreserved embryos, depending on the number of days between oocyte retrieval and cryopreservation of the embryo.

Material

The sonographic volumes were acquired using a Voluson E8 ultrasound machine (GE Medical Systems, Zipf, Austria) and obtained with a transvaginal scan (GE-probe RIC-6-12-D [4.5–11.9 MHz]). With regard to the safety aspects of first trimester ultrasound the thermal index (TI) and mechanical index (MI) were kept below 1.0, the examiners were qualified and experienced, and the as-low-as-reasonable-practicable (ALARP) principle was respected: the duration of the examination did not exceed 30 minutes, and 3D images were stored for offline evaluation in order to reduce the exposure to ultrasound as much as possible.[15] The 3D datasets were collected when the foetus was at rest. The 3D volumes were transferred to the BARCO I-Space (Barco N.V., Kortrijk, Belgium) and visualised in 3D using our V-Scope software.[16] The hologram, visualised through polarising glasses, can be manipulated by a wireless joystick tracked by an optical tracking system. This joystick also controls a measuring tool to trace lines and measure angles and volumes. For our study the 3D volumes were resized (enlarged), rotated and cropped when necessary and grey-scale and opacity values were adjusted for optimal image quality.

Measurements

We measured the frontal angle, being a measure for plantar flexion of the foot, between the ventral side of the lower leg and the ventral side of the foot by drawing a line from the ventral side of the knee joint to the instep and a line from the instep to the end of the middle toe using the joystick. The computer calculated the angle between both lines. Thereafter we measured the lateral angle, being a measure for adduction of the foot, between the lateral side of the leg and the lateral side of the foot by drawing a line from the lateral side of the fifth to the medial side of the first toe and a line from the medial side of the first toe upwards and parallel in all directions to the lower leg, using the line of the first measurement as a reference (**Figure 2**). The possibility to draw this line is a unique feature of virtual reality, which offers the opportunity to check for parallelism in all directions. The measurement procedure was, when possible, performed separately for both feet and in that case the difference between both feet was calculated as well.

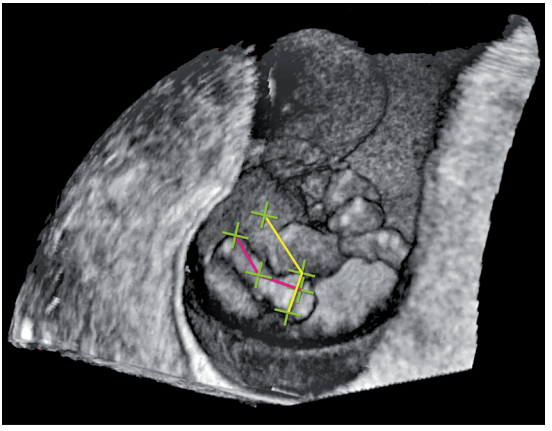

Figure 2: measurements on the foetal foot performed in the I-Space;
- frontal angle: a line from the ventral side of the knee joint to the instep and a line from the instep to the end of the middle toe (pink line)
- lateral angle: a line from the lateral side of the fifth to the medial side of the first toe and a line from the medial side of the first toe upwards and parallel in all directions to the lower leg (yellow line)

Statistical analysis

Interclass and intraclass correlations were calculated from a two way model using R 2.51.1.[17] Reference curves were estimated using the GAMLSS package.[18] For each outcome curves were fitted using a normal, scaled t and the Box-Cox transformed normal and several numbers of degrees of freedom in the splines for the location and dispersion were tried[19] and the best fitting model was selected using the Akaike Information Criterion (AIC). The AIC is a measure for the goodness-of-fit of a model that corrects for model complexity. By using the model with the best AIC we made sure that we selected a well-fitting model that is not more complex than necessary. Here we treated the data as if all observations were independent (since no standard methods for reference curves correlated observations exist).

Reproducibility

All measurements were performed offline and for each angle measurement 30 randomly chosen measurements, by using a numeric computer-generated sequence, were repeated by the same observer (MR) and the same 30 measurements were measured by another observer (HB) to determine reproducibility. The measurements used for intra- and interobserver analysis were performed after an interval of at least two weeks.

Results

From the 112 pregnancies 530 volumes were obtained for evaluation. Patient characteristics and success rates are presented in **Table 1 and 2** respectively.

The measurements of the angles are plotted against the GA in **Figure 3**. Both curves of the right and left foot look similar, showing the same pattern for both frontal and lateral angles. Regarding the frontal angles of the left and right foot, a decrease of the angle with advancing GA is observed from approximately 155 to 110 degrees. However, the lateral angles show a different curve: the angles first increase from approximately 105 to 125

Characteristic	Median (range) or percentage
Mothers (n=112)	
Maternal age (years)	32.9 (18.9-42.7)
Gravidity	2 (1-10)
Parity	
0	62.5%
1	27.7%
≥ 2	9.8%
Miscarriages ≥ 2	25.9%
Conception mode	
Natural	70.5%
IVF or IVF/ICSI	27.7%
Intrauterine insemination	1.8%
Gestational diabetes	5.4%
Hypertensive disorders	8.9%
Foetal growth restriction	3.6%
Newborns (n=112)	
Female	52.7%
Birth weight (grams)	3390 (450-4700)
GA at delivery (weeks)	39+4 (26+4 to 42+0)

Table 1: general characteristics
IVF: in vitro fertilisation, ICSI: intracytoplasmic sperm injection, GA: gestational age

Week	Right leg	%	Left leg	%
8	14/104	13.5	16/104	15.4
9	28/109	25.7	25/109	22.9
10	56/108	51.9	53/108	49.1
11	69/108	63.9	58/108	53.7
12	40/101	39.6	37/101	36.6

Table 2: success percentages of angle measurements (measurements/number of images; %) by gestational age (expressed in complete weeks)

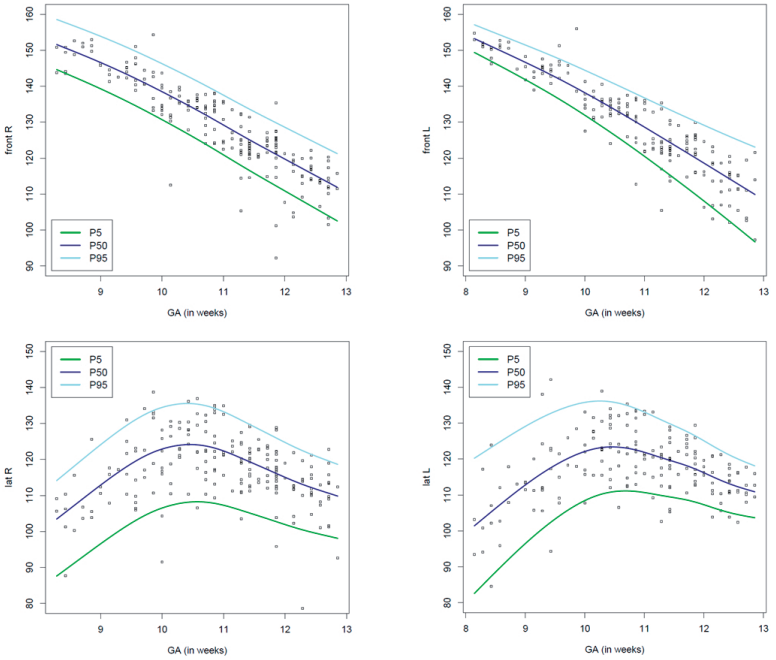

Figure 3: individual measurements of
upper left: the frontal angle of the right foot (using TF: t-family)
upper right: the frontal angle of the left foot (using TF: t-family)
lower left: the lateral angle of the right foot (using BCCG: Box-Cox Cole and Green)
lower right: the lateral angle of the left foot (using NO: Normal)

degrees and reach a peak at about 11 weeks GA, resulting in a physiological clubfoot position, followed by a decrease to 110 degrees thereafter. The lateral curves flatten from 12 weeks GA onwards and a continuing decrease is observed thereafter. Left and right differences of frontal and lateral angles in the same cases are depicted in **Figure 4**. No preponderance of left or right feet is observed. Differences in frontal angles appeared to be smaller than in lateral angles.

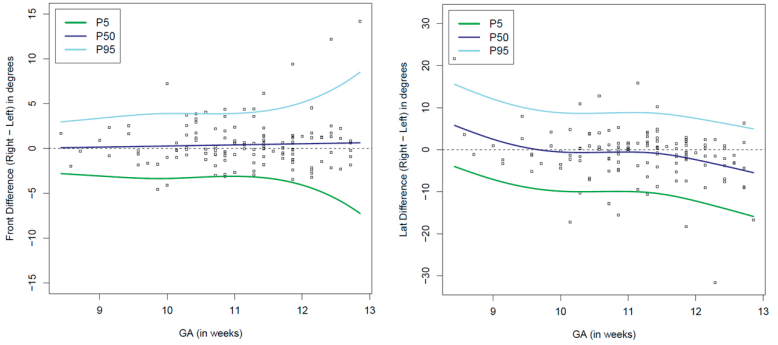

Figure 4: left and right differences of frontal and lateral angles in the same cases; outliers belong to different foetuses

Reproducibility was good. The mean differences, the 95% limits of agreement and the intraclass correlation coefficients (ICC) of intra- and interobserver variability are shown in **Table 3**. Bland- and Altman plots are shown in **Figures 5 and 6**.

	mean difference (degrees)	**95% limits of agreement (degrees)**	**ICC**
intra observer variability			
left frontal	-0.34	-2.81 to 2.14	0.995
right frontal	-0.55	-3.07 to 1.97	0.994
left lateral	-0.23	-2.26 to 1.79	0.986
right lateral	-0.15	-2.9 to 2.6	0.985
inter observer variability			
left frontal	0.14	-10.56 to 10.85	0.935
right frontal	0.33	-9.28 to 9.95	0.941
left lateral	-0.39	-6.38 to 5.60	0.872
right lateral	0.57	-6.17 to 7.32	0.909

Table 3: reproducibility
ICC: intraclass correlation coefficient

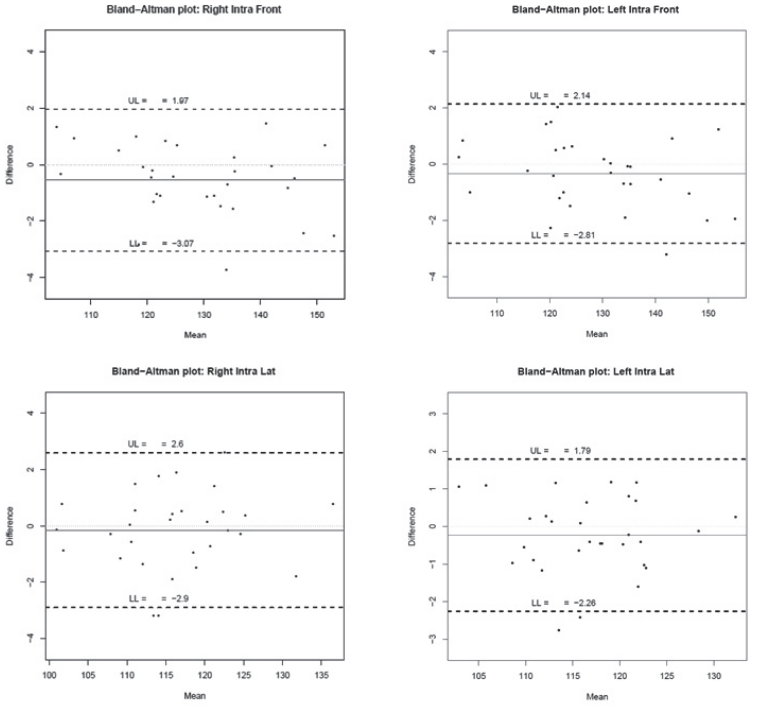

Figure 5: Bland and Altman-plots showing the intra-observer variability of the four different angles; UL: upper limit, LL: lower limit, both of the 95% limits of agreement, mean and difference both in degrees

Discussion

We investigated the foetal development of the lower limb by means of virtual reality and succeeded in measuring the first trimester physiological clubfoot in vivo objectively. Our findings are consistent with the in vitro study on development of the legs and feet of Victoria-Diaz and Victoria-Diaz, who described the changes in the foot position of embryos from legal abortions already three decades ago (**Figure 7**).[10] In the first stage of development

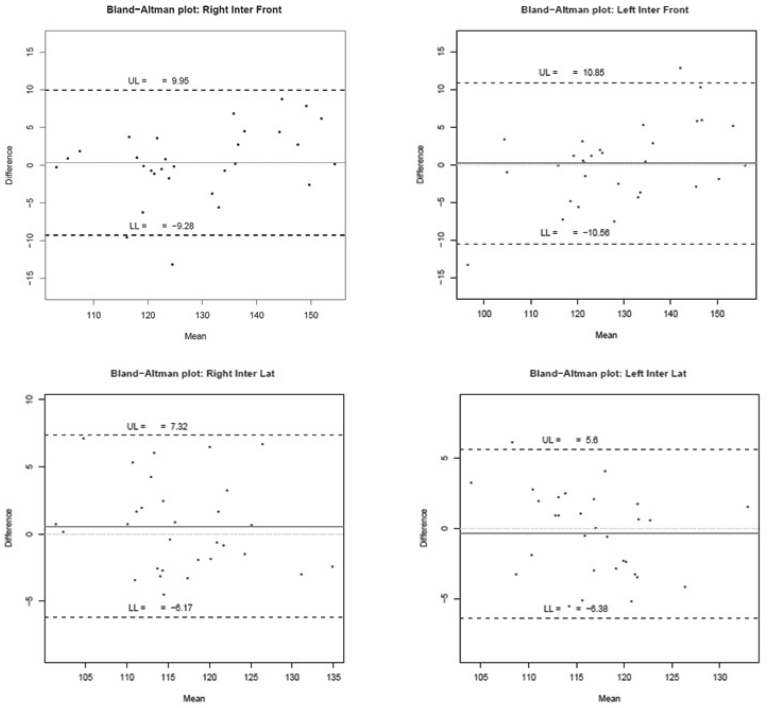

Figure 6: Bland and Altman-plots showing the inter-observer variability of the four different angles; UL: upper limit, LL: lower limit, both of the 95% limits of agreement, mean and difference both in degrees

the foot is in line with the leg. Because of the relatively large growth of the fibula compared to the tibia, in the second stage the foot is displaced in inversion and dorsiflexion, resulting in a physiological clubfoot ('fibular phase'). The fibular phase is observed when the length of the embryo is 21-30 mm, which roughly corresponds to 8.5-10 weeks GA. In the third stage growth acceleration of the tibia causes the foot to attain its normal position ('tibial phase'). The embryonic length is 31-50 mm during the tibial phase, which roughly corresponds to 10-11.5 weeks GA. At this early stage

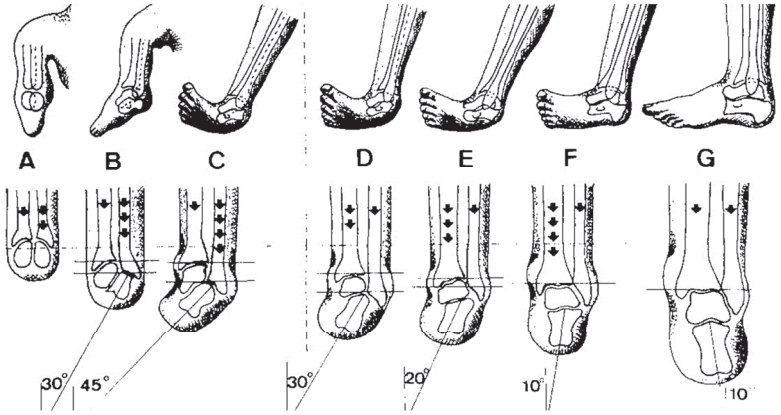

Figure 7: embryonic development of the lower limb, derived from earlier publication[10], reprinted with permission from the publisher

of pregnancy the length of the fibula and tibia cannot be reliable measured with ultrasound as the bones mainly consist of less echogenic cartilage. However, since it is possible to measure the angles of the foot position, using virtual reality the observation of a transient clubfoot position in our study is confirmed. The lateral angles of the feet first increase, which corresponds to the fibular phase (**Figure 8**). Next the lateral angles decrease again to attain a normal foot position, corresponding to the tibial phase. It is assumed that failure to move on from the fibular to the tibial phase results in a congenital clubfoot.

Another anatomical study was performed by Kawashima and Uhthoff: they investigated in vitro 189 feet in foetuses ranging from 9 to 22 weeks GA.[20] They observed a steady decline in the frontal angle until the end of 12 weeks GA as well. From 13 weeks GA, no changes in foot position were observed. The lateral angle first increased until 11 weeks GA followed by a decrease thereafter. Changes in foot position during the physiological clubfoot occurred mainly at the talar level and they concluded that clubfeet might be

Figure 8: physiological clubfoot at 10 weeks and 2 days gestational age

caused by a developmental arrest of the talus. Regardless of aetiology, the changes in foot position are the same and correspond with our results.

The hypothesis that clubfeet are caused by a growth disturbance is sustained by Dietz.[21] He explained this by the differences in muscle fibres and cellular content in the lower leg in patients with clubfeet, possibly caused by a regional abnormality of the tibial nerve.

Duce et al. investigated clubfeet in mice by means of micro magnetic resonance imaging (MRI).[22] The *peroneal muscle atrophy* (*pma*) mouse mutant has, due to atrophy of the anterior and lateral muscle compartments in

the hind limbs, a clubfoot position. Although several differences in anatomy between this mutant mouse and humans affected by congenital clubfoot are seen, the authors observed an arrest in the development of the hind foot. This development was not completed in *pma* mice compared to the wild type, suggesting a comparable aetiology of this anomaly.

Over the years congenital clubfeet are increasingly detected using prenatal ultrasound,[6, 23] although there remains a false positive diagnosis in about 10% of the cases.[24] Glotzbecker et al. tried to decrease this by using a 2D angle measurement classification system. In a sagittal view the angle between the long-axis of the leg respectively the foot (resembling our 'lateral angle') was measured. False positive rate dropped dramatically using a cut off of 80 degrees.[25] Grande et al. performed a large (n=13,723) retrospective study to assess sensitivity of detecting anomalies in the first trimester. They found an overall detection rate for minor skeletal anomalies like clubfeet of only 9%.[26] Our data show that an isolated clubfoot position suspected at the time of the nuchal translucency scan might be a transient finding.

Our results gain more insight in the normal development of the foot position and its sonographic appearance, being a prerequisite for diagnosing abnormalities like a pathological clubfoot. Further research is required to determine the foot position in foetuses in the first trimester that later on appear to have a congenital clubfoot. Continuation of collection of first trimester volumes might include foetuses, which later appear to be affected by clubfeet. This will allow comparison of normal to abnormal foot position and increase our understanding of the development and aetiology of this common anomaly.

To our best knowledge, we are the first to measure the foot position in vivo using ultrasound.

The characteristics of this subgroup are comparable to those of women enrolled between 2010 and 2014.[27] The approach we used in this study

appeared to be a reproducible technique to evaluate the foetal foot position in early pregnancy.

The observed differences between right and left feet (**Figure 4**) could be caused by a difference in growth or development between the right and left foot in individual cases. Limbs develop in a craniocaudal fashion but we are not aware of a left-right or right-left gradient. We are yet not able to explain this difference, albeit small.

The proposed angle measurement technique cannot be carried out using ultrasound equipment with a 2D display, limiting its applicability. However, specialised 3D software is available to perform angle measurements on ultrasound machines or desktop computers. Also a user friendly and cheap 3D VR desktop system has been developed for routine use of diagnostic 3D VR ultrasound on a separate non-expensive desktop computer in an outpatient clinic, allowing precise length, volume and angle measurements.[28]

A limitation is that only data were available until 13 weeks GA. The still decreasing lateral angles at the end of 12 weeks GA suggest a continuing developing foot position, although Kawashima and Uhthoff did not observe this in their anatomical studies. Although a foetus with a congenital club-foot has not been observed in our study, it seems reasonable to defer the prenatal diagnosis of this anomaly to at least a GA of more than 13 weeks.

Another limitation is the low success rate of the angle measurements, especially at 8 and 9 weeks GA, possibly due to the relatively small foetal extremities at that moment. (**Table 2**). Although ultrasound generally is regarded as a safe instrument to use in early pregnancy, in order to keep the exposure to ultrasound as short as possible, in our study only already stored non-targeted 3D sweeps of the entire foetus were used. This may have hampered the quality of the volumes we acquired. Dedicated volume acquisition of the foetal feet might result in higher feasibility figures. Also movement artefacts of the foetus could have impeded accurate visualisation. All these aspects contributed to the suboptimal success rate.

By using 3D virtual reality, we have succeeded to develop a measurement tool for objective foot position assessment and to create reference data for the first trimester foot position. The angle measurements would not have been possible without the use of this innovative technique. A transient clubfoot position is present during the normal development of the lower limbs and it has been measured in vivo for the first time. Our data show that in early pregnancy a clubfoot may be physiological and diagnosis of a pathological clubfoot should be deferred to the second trimester.

Acknowledgments

We would like to thank Mr Tom de Vries Lentsch for his help with processing **Figure 2** and **Figure 8**.

References

1. Syngelaki A, Chelemen T, Dagklis T, Allan L, Nicolaides KH. Challenges in the diagnosis of fetal non-chromosomal abnormalities at 11-13 weeks. Prenat Diagn. 2011;31(1):90-102.
2. Chaoui R, Nicolaides KH. Detecting open spina bifida at the 11-13-week scan by assessing intracranial translucency and the posterior brain region: mid-sagittal or axial plane? Ultrasound Obstet Gynecol. 2011;38(6):609-12.
3. Steegers-Theunissen RP, Steegers EA. Embryonic health: new insights, mHealth and personalised patient care. Reprod Fertil Dev. 2015;27(4):712-5.
4. Werler MM, Yazdy MM, Mitchell AA, Meyer RE, Druschel CM, Anderka M, et al. Descriptive epidemiology of idiopathic clubfoot. Am J Med Genet A. 2013; 161A(7):1569-78.
5. Miedzybrodzka Z. Congenital talipes equinovarus (clubfoot): a disorder of the foot but not the hand. J Anat. 2003;202(1):37-42.
6. Offerdal K, Jebens N, Blaas HG, Eik-Nes SH. Prenatal ultrasound detection of talipes equinovarus in a non-selected population of 49 314 deliveries in Norway. Ultrasound Obstet Gynecol. 2007;30(6):838-44.
7. Bakalis S, Sairam S, Homfray T, Harrington K, Nicolaides K, Thilaganathan B. Outcome of antenatally diagnosed talipes equinovarus in an unselected obstetric population. Ultrasound Obstet Gynecol. 2002;20(3):226-9.
8. Cohen-Overbeek TE, Grijseels EW, Lammerink EA, Hop WC, Wladimiroff JW, Diepstraten AF. Congenital talipes equinovarus: comparison of outcome between a prenatal diagnosis and a diagnosis after delivery. Prenat Diagn. 2006; 26(13):1248-53.
9. Sanzarello I, Nanni M, Faldini C. The clubfoot over the centuries. J Pediatr Orthop B. 2017;26(2):143-51.
10. Victoria-Diaz A, Victoria-Diaz J. Pathogenesis of idiopathic clubfoot. Clin Orthop Relat Res. 1984(185):14-24.
11. Baken L, van Heesch PN, Wildschut HI, Koning AH, van der Spek PJ, Steegers EA, et al. First-trimester crown-rump length and embryonic volume of aneuploid fetuses measured in virtual reality. Ultrasound Obstet Gynecol. 2013;41(5): 521-5.
12. Gijtenbeek M, Bogers H, Groenenberg IA, Exalto N, Willemsen SP, Steegers EA, et al. First trimester size charts of embryonic brain structures. Hum Reprod. 2014;29(2):201-7.

13. Baken L, Benoit B, Koning AHJ, van der Spek PJ, Steegers EAP, Exalto N. First-Trimester Crown-Rump Length and Embryonic Volume of Fetuses with Structural Congenital Abnormalities Measured in Virtual Reality: An Observational Study. Biomed Res Int. 2017;2017:1953076.

14. Steegers-Theunissen RP, Verheijden-Paulissen JJ, van Uitert EM, Wildhagen MF, Exalto N, Koning AH, et al. Cohort Profile: The Rotterdam Periconceptional Cohort (Predict Study). Int J Epidemiol. 2016;45(2):374-81.

15. Knez J, Day A, Jurkovic D. Ultrasound imaging in the management of bleeding and pain in early pregnancy. Best Pract Res Clin Obstet Gynaecol. 2014;28(5): 621-36.

16. Rousian M, Exalto N, Koning A, Steegers EAP. Three-Dimensional Virtual Reality in Early Pregnancy. In: Farquharson RG, Stephenson MD, editors. Early Pregnancy. Second Edition. ed: Cambridge University Press.; 2017. p. 208-19.

17. RCoreTeam. R: A language and environment for statistical computing: R Foundation for Statistical Computing, Vienna, Austria; 2015 [Available from: http://www.R-project.org.

18. Rigby RA, Stasinopoulos DM. Generalized additive models for location, scale and shape. J Roy Stat Soc C-App. 2005;54:507-44.

19. Hastie T. Generalized additive models. In: Chambers&Hastie, editor. Statistical Models in S: Wadsworth & Brooks/Cole; 1992.

20. Kawashima T, Uhthoff HK. Development of the foot in prenatal life in relation to idiopathic club foot. J Pediatr Orthop. 1990;10(2):232-7.

21. Dietz FR. On the pathogenesis of clubfoot. Lancet. 1985;1(8425):388-90.

22. Duce S, Madrigal L, Schmidt K, Cunningham C, Liu G, Barker S, et al. Micro-magnetic resonance imaging and embryological analysis of wild-type and pma mutant mice with clubfoot. J Anat. 2010;216(1):108-20.

23. Liao YM, Li SL, Luo GY, Wen HX, Ouyang SY, Chen CY, et al. Routine screening for fetal limb abnormalities in the first trimester. Prenat Diagn. 2016;36(2):117-26.

24. Lauson S, Alvarez C, Patel MS, Langlois S. Outcome of prenatally diagnosed isolated clubfoot. Ultrasound Obstet Gynecol. 2010;35(6):708-14.

25. Glotzbecker MP, Estroff JA, Spencer SA, Bosley JC, Parad RB, Kasser JR, et al. Prenatally diagnosed clubfeet: comparing ultrasonographic severity with objective clinical outcomes. J Pediatr Orthop. 2010;30(6):606-11.

26. Grande M, Arigita M, Borobio V, Jimenez JM, Fernandez S, Borrell A. First-trimester detection of structural abnormalities and the role of aneuploidy markers. Ultrasound Obstet Gynecol. 2012;39(2):157-63.

27. Parisi F, Rousian M, Koning AH, Willemsen SP, Cetin I, Steegers EA, et al. Periconceptional maternal biomarkers of one-carbon metabolism and embryonic growth trajectories: the Rotterdam Periconceptional Cohort (Predict Study). Fertil Steril. 2017;107(3):691-8 e1.

28. Baken L, van Gruting IM, Steegers EA, van der Spek PJ, Exalto N, Koning AH. Design and validation of a 3D virtual reality desktop system for sonographic length and volume measurements in early pregnancy evaluation. J Clin Ultrasound. 2015;43(3):164-70.

CHAPTER 5

Accuracy of foetal sex determination in the first trimester of pregnancy using 3D virtual reality ultrasound

Bogers H, Rifouna MS, Koning, AHJ, Husen-Ebbinge M, Go ATJI, Spek PJ van der, Steegers-Theunissen RPM, Steegers EAP, Exalto N.

J Clin Ultrasound. 2018 May;46(4):241-246

Abstract

Purpose: Early detection of foetal sex is becoming more popular. The aim of this study was to evaluate the accuracy of foetal sex determination in the first trimester, using 3D virtual reality.

Methods: 3D ultrasound volumes were obtained in 112 pregnancies between 9 and 13 weeks gestational age, offline projected as a hologram in the BARCO I-Space and subsequently the genital tubercle angle was measured. Separately, the 3D aspect of the genitalia was examined for having a male or female appearance.

Results: Although a significant difference in genital tubercle angles was found between male and female foetuses it did not result in a reliable prediction of foetal gender. Correct sex prediction based on first trimester genital appearance was at best 56%.

Conclusion: Our results indicate that accurate determination of the foetal sex in the first trimester of pregnancy is not possible, even by using an advanced 3D ultrasound technique.

Introduction

Prenatal detection of the foetal sex can be important for medical reasons, such as inherited diseases, e.g., in case of X-linked diseases like Duchenne muscular dystrophy.

Ultrasonographic foetal sex determination is usually performed during the Foetal Anomaly Scan at 18 - 22 weeks gestational age (GA). The reported accuracy ranges between 92 and 100%.[1] With help of the "sagittal sign" in the midline sagittal plane, foetal sex determination is accurate in almost 100% of cases with normal external genitalia after 13 weeks of pregnancy. The differentiation is based on the identification of a "dome sign", representing foetal penis and scrotum, or two or four parallel lines representing labia majora and minora.[2] Not all ultrasonographers are aware of the pitfall that during routine ultrasound before 13 weeks of pregnancy a pronounced genital tubercle of a female foetus may resemble a penis. In the first trimester of pregnancy, the external genitalia of both male and female foetuses appear the same: two labio-scrotal folds with a genital tubercle in the upper midline. In the presence of testes these structures are transformed into a male scrotum and penis respectively. Without the induction by the testes, these structures become the default female labia majora and clitoris.[2]

The angle between the genital tubercle and the body axis has been suggested as a useful in vivo ultrasound parameter for foetal sex determination between 11 and 14 weeks of pregnancy.[3] Male foetuses display a cranially directed tubercle whereas in female foetuses the tubercle is pointed caudally ('sagittal sign'). However, most research in the first trimester has been performed by means of two-dimensional ultrasound[4-7] and at a relatively late GA of more than 11 weeks.[3, 8] Moreover, concerns have been raised about the possibility of determining the sex at an early stage. It has been observed that the genital tubercle angle can change during ultrasonographic examination, caused by an erectile displacement, already at 11 weeks GA.[9]

Recent developments in three-dimensional (3D) ultrasonographic imaging techniques have resulted in improved visualisation of the developing foetus.

A new visualisation approach, based on a 3D virtual reality (3D VR) environment, allows depth perception and interaction with the volume-rendered (ultrasound) data in a more natural and intuitive way compared to 3D images displayed on a 2D screen. This 3D VR approach improves an early detection of surface abnormalities and has already successfully been used in the determination of ambiguous genitalia in a later stage of pregnancy.[10, 11]

Although the foetal genitalia have not been developed entirely, we wanted to investigate whether foetal sex could ultrasonographically be predicted before 13 weeks of pregnancy using a very advanced ultrasound technique. The aim of this study was to evaluate accuracy of foetal sex determination between 9 and 12 weeks of pregnancy, using not only the genital tubercle angle measurement but also a qualitative assessment of the genitalia by means of 3D ultrasound. A secondary aim was to determine the reproducibility of the genital tubercle angle measurement in this early period of pregnancy.

Materials and Methods

Study population

This study comprises women participating in a study on first trimester longitudinal 3D ultrasound measurements conducted at a university hospital to evaluate foetal growth and development using new imaging techniques. Pregnant women who participated were enrolled via the outpatient clinic of the department of Obstetrics and Gynaecology and local midwifery practices. All women received weekly 3D ultrasound scans between 6+0 and 12+6 weeks GA. Only women less than eight weeks pregnant with a singleton pregnancy entered the study for further analysis.

In 2009 we enrolled 141 women from whom at least one volume was obtained in our study. Two pregnancies complicated with trisomy 21 and three with congenital anomalies were excluded. Three multiple pregnancies, three drop outs, 16 miscarriages and two cases with an intrauterine foetal demise had to be excluded as well, leaving 112 inclusions for analysis (**Figure 1**).

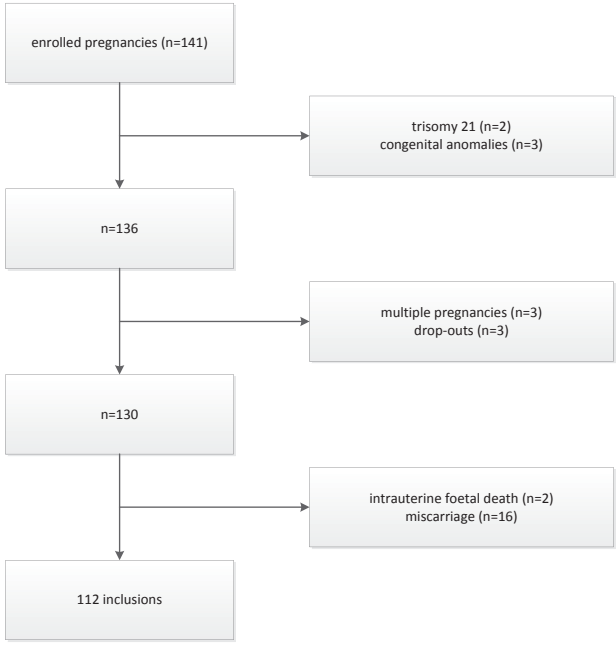

Figure 1: flowchart illustrating inclusions and exclusions of the study population

Ethical approval

All participants signed a written informed consent form and the local medical and ethical review committee approved the study protocol (METC 232.394/2003/177, METC 323.395/2003/178, MEC 2004–227).

Pregnancy dating

The GA was calculated according to the first day of the last menstrual period (LMP) in case of a regular menstrual cycle of 28 days and adjusted for a longer or shorter cycle.[12] In case of a discrepancy in GA of more than seven days between crown rump length (CRL) and the last menstrual period (LMP), or an unknown LMP, the GA was calculated by using CRL at the end of the first trimester. In case of assisted reproductive technology, GA

was determined by the date of oocyte retrieval plus 14 days in pregnancies conceived via in vitro fertilisation with or without intracytoplasmic sperm injection (IVF/ICSI) procedures, from the LMP or insemination date plus 14 days in pregnancies conceived through intrauterine insemination, and from the day of embryo transfer plus 17 or 18 days in pregnancies originating from the transfer of cryopreserved embryos, depending on the number of days between oocyte retrieval and cryopreservation of the embryo.

Material

The ultrasonographic volumes were acquired using a Voluson E8 ultrasound machine (GE Medical Systems, Zipf, Austria) and obtained with a transvaginal scan (GE-probe RIC-6-12-D [4.5–11.9 MHz]). With regard to the safety aspects of first trimester ultrasound the thermal index (TI) and mechanical index (MI) were kept below 1.0, the examiners were qualified and experienced, and the as-low-as-reasonable-practicable (ALARP) principle was respected: the duration of the examination did not exceed 30 minutes, and 3D images were stored for offline evaluation in order to reduce the exposure to ultrasound as much as possible.[13] The 3D volumes were converted to a Cartesian format and visualised in the BARCO I-Space (Barco N.V., Kortrijk, Belgium). This is a four-walled CAVE™-like (Cave Automatic Virtual Environment) virtual reality system. Observers are immersed in a virtual reality room, surrounded by computer-generated passive stereo images, which are projected by eight projectors onto three walls and the floor of a small room. The V-Scope volume-rendering application is used to create a 'hologram' of the ultrasound volume that is being investigated, floating in space in front of the observer. The hologram is viewed through polarising glasses, similar to those used to view 3D movies, to create the perception of depth. The hologram can be manipulated by means of a virtual pointer, controlled by a wireless joystick. This joystick also operates a measuring tool to trace lines and measure angles and volumes. In addition tracking of the viewer's head allows the computer to provide the correct perspective and motion parallax, which in combination with the stereoscopic images, helps in discerning fine details and in the understanding of 3D structures in the volumes. For our study the 3D volumes were resized (enlarged), rotated and cropped when necessary and grey-scale and opacity values were adjusted for optimal image quality.[14, 15]

Measurements

In the BARCO I-Space the 3D foetal hologram was placed in a horizontal position and callipers were placed in a mid-sagittal cross section for a very precise CRL measurement. A second line was positioned in the central axis of the genital tubercle and the angle between the genital tubercle and the CRL line, being the central bodyline, was measured[3] (**Figure 2**). Because of a more precise positioning of the callipers we measured the angle between the tubercle and the upper part of the CRL line. The genital tubercle angle was calculated afterwards by subtracting the measured angle from 180 degrees.

Apart from this quantitative prediction, two experienced ultrasonographers (MHE and NE) examined the foetal genitalia for a male or female appearance separately without knowing their results or the duration of pregnancy. All volumes in which an angle measurement had been performed were projected in the BARCO I-Space and were scored as male, female or unknown. All examiners were blinded for the outcome of pregnancy. After all measurements had been performed the results were compared to the neonatal sex at birth as reference.

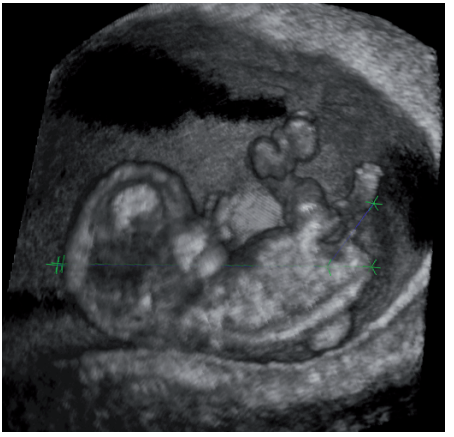

Figure 2: measurement of the genital tubercle angle of a male foetus at a GA of 10 weeks and 2 days in the BARCO I-Space

Statistical analysis

The measured angle by GA was described with ordinary least squares regression analysis for male and female foetuses separately. The dependent variable was measured angle; the independent variables were GA and square of GA.

Predictive accuracy of foetal sex was evaluated with binary logistic regression, with foetal sex as dependent variable and GA, square of GA, measured angle and square of measured angle as independent variables (backward conditional analysis). Predictive value was assessed as the proportion of correct predictions. A $p<0.05$ (two-sided) was considered a statistically significant difference.

Reliability of the measurements was depicted with Bland Altman plots indicating the bias (the systematic of mean difference between two measurements) and limits of agreement (LOAs). Intraclass correlation coefficients (ICCs, two way mixed, single measures, absolute agreement) of intraobserver and interobserver angle measurements were added.

Reliability of the qualitative prediction was determined by calculating Cohen's kappa. We used the directives of reproducibility as described by Landis and Koch[16] (poor: $\kappa<0$; slight: $\kappa=0.00–0.20$; fair: $\kappa=0.21– 0.40$; moderate: $\kappa=0.41–0.60$; substantial: $\kappa=0.61–0.80$; almost perfect $\kappa>0.80$).

Reproducibility

All measurements were performed offline. Intrarater agreement was assessed by single repeated measurement of 30 randomly selected volumes (16 male, 14 female) by the same examiner (HB). Interrater agreement was evaluated by comparing the measurements of the same 30 volumes performed by another examiner (MR).

Results

From the 112 pregnancies 426 volumes were obtained for evaluation from 9 until 13 weeks GA. Median maternal age was 32.9 years (range: 18.9-42.7). 62.5% were nulliparous and 25.9% had a history of two or more miscarriages. 70.5% conceived naturally. Median birth weight was 3390 grams (range: 450-4700) and median GA at delivery was 39 weeks + 4 days (range: 26+4 - 42+0) (**Table 1**). No anomalies of the genitalia were observed postpartum.

In 102 out of 112 singleton pregnancies at least one measurement was feasible, concerning 53 male (range 9+0 - 12+6 weeks+days GA) and 59

Characteristic	**Median (range) or percentage**
Mothers (n=112)	
Maternal age (years)	32.9 (18.9-42.7)
Gravidity	2 (1-10)
Parity	
0	62.5%
1	27.7%
≥ 2	9.8%
Miscarriages ≥ 2	25.9%
Conception mode	
Natural	70.5%
IVF or IVF/ICSI	27.7%
Intrauterine insemination	1.8%
Gestational diabetes	5.4%
Hypertensive disorders	8.9%
Foetal growth retardation	3.6%
Newborns (n=112)	
Female	52.7%
Birth weight (grams)	3390 (450-4700)
GA at delivery (weeks)	39+4 (26+4 to 42+0)

Table 1: general characteristics of the study population
IVF: in vitro fertilisation, ICSI: intracytoplasmic sperm injection, GA: gestational age

female (range 9+0 - 12+6 weeks+days GA) foetuses. A genital tubercle angle measurement could be measured in 235 of 426 3D volumes (total 55.2%; male: 116/206=56.3%, female: 119/220=54.1%). The feasibility per pregnancy week is described in **Table 2**. The median number of angle measurements was 2 (range: 1-4) for male as well as female foetuses. **Table 3** displays the regression lines corresponding to the pattern seen in male and female foetuses.

Figure 3 points to a considerable overlap between the measurements of male and female foetuses. The curves follow more or less the same trend between 60 and 80 days GA, but from then (approximately 11 weeks GA) onwards a different pattern is seen: the mean angle of male foetuses increases

Week	Male	%	Female	%	Total	%
9	26/54	48.1	25/54	46.3	51/108	47.2
10	31/54	57.4	41/55	74.5	72/109	66.1
11	36/50	72.0	37/58	63.8	73/108	67.6
12	23/48	47.9	16/53	30.2	39/101	38.6
Total	116/206	56.3	119/220	54.1	235/426	55.2

Table 2: success percentages of genital tubercle angle measurements for male- and female foetuses (number of feasible measurements / number of available volumes; %) by gestational age (expressed in complete weeks)

	Male Beta-coefficient (95%CI of beta-coefficient)	P	Female Beta-coefficient (95%CI of beta-coefficient)	P
Constant	627.13 (40.98 ; 1213.27)	0.04	189.73 (-357.24 ; 736.70)	0.49
Gestational age (days)	-14.24 (-30.22 ; 1.74)	0.08	-1.48 (—16.42 ; 13.45)	0.84
Square of gestational age	0.09 (-0.02 ; 0.20)	0.11	-0.00 (-0.11 ; 0.10)	0.94
Adjusted R^2	0.23		0.41	
P of regression		<0.001		<0.001

Table 3: relationship between measured angle and gestational age for male and female foetuses separately
CI: confidence interval

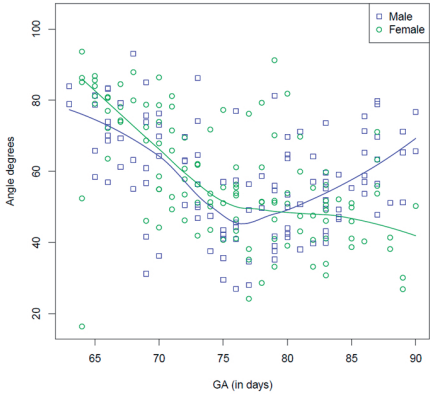

Figure 3: scatterplot of measured genital tubercle angles (circles: female foetuses, squares: male foetuses) against gestational age; the curves represent the fitted regression curves (green line: female foetuses, blue line: male foetuses)

whereas the mean angle of female foetuses slightly diminishes. GA, square of GA, measured angle and square of measured angle were not significantly associated with a correct prediction of foetal sex. The power to predict sex was moderate, only 54.9% of measurements were correctly predicted (**Table 4**). The receiver operating characteristic (ROC) curve is shown in **Figure 4**.

Table 5 displays the results of the qualitative prediction, based on the genital appearance, per gestational week. Correct prediction was at best 56.4% (range: 28.8%-56.4%). **Figure 5** illustrates a pronounced genital tubercle in a female foetus. In 6.9%-23.0% of the cases foetal sex prediction was not possible, although angle measurements in these cases were feasible.

With regard to the angle measurements the Bland and Altman plots are shown in **Figures 6** (intraoperator agreement) and **7** (interoperator agreement). Reproducibility was excellent. The intraclass correlation coefficients of intra- and interoperator angle measurements were 0.97 (95% confidence interval [CI]: 0.94 - 0.99) and 0.95 (95% CI: 0.90-0.98), respectively.

The measure of agreement of the qualitative sex prediction was fair: κ = 0.24 (95% CI: 0.13-0.34) with the prediction 'unknown' taken into account.

	OR	95%CI of OR	P
Constant	$2.35 \cdot 10^{-4}$		0.78
Gestational age (days)	1.37	0.27 ; 7.29	0.70
Square of gestational age	1.00	1.00 ; 1.01	0.71
Angle (degrees)	0.87	0.73 ; 1.02	0.11
Square of angle (degrees)	1.00	1.00 ; 1.00	0.09
Proportion correct predictions	54.9%	45.2 ; 64.6	
Area under the curve	0.61	0.50 ; 0.72	

Table 4. Logistic regression analysis, backward conditional analysis.
OR: odds ratio. CI: confidence interval.

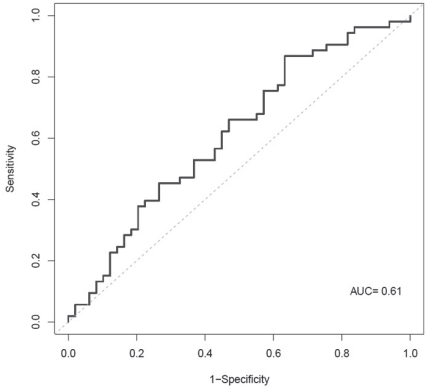

Figure 4: receiver operating characteristic (ROC) curve of foetal sex determination by measuring the genital tubercle angle

Discussion

Although the relation between genital tubercle angle measurement and GA differs significantly between male and female foetuses, our results indicate that prediction of the foetal sex by measuring the angle of the genital tubercle in the first trimester of pregnancy before 12 weeks GA in individual cases was not reliable. Furthermore, prediction of the foetal sex based on genital appearance in this period was at best 56.4%.

GA (weeks)	Rater 1			Rater 2			Total
	True	False	Unknown	True	False	Unknown	
9	15 (28.8%)	31 (59.6%)	6 (11.5%)	22 (42.3%)	22 (42.3%)	8 (15.4%)	52
10	38 (52.8%)	29 (40.3%)	5 (6.9%)	32 (44.4%)	32 (44.4%)	8 (11.1%)	72
11	35 (47.3%)	28 (37.8%)	11 (14.9%)	31 (41.9%)	26 (35.1%)	17 (23.0%)	74
12	17 (43.6%)	16 (41.0%)	6 (15.4%)	22 (56.4%)	10 (25.6%)	7 (17.9%)	39

Table 5: the results of foetal sex prediction by determining a male or female appearance of the genitalia in the Barco I-Space
True: correct prediction of foetal sex. False: wrong prediction of foetal sex. Unknown: prediction was not possible.

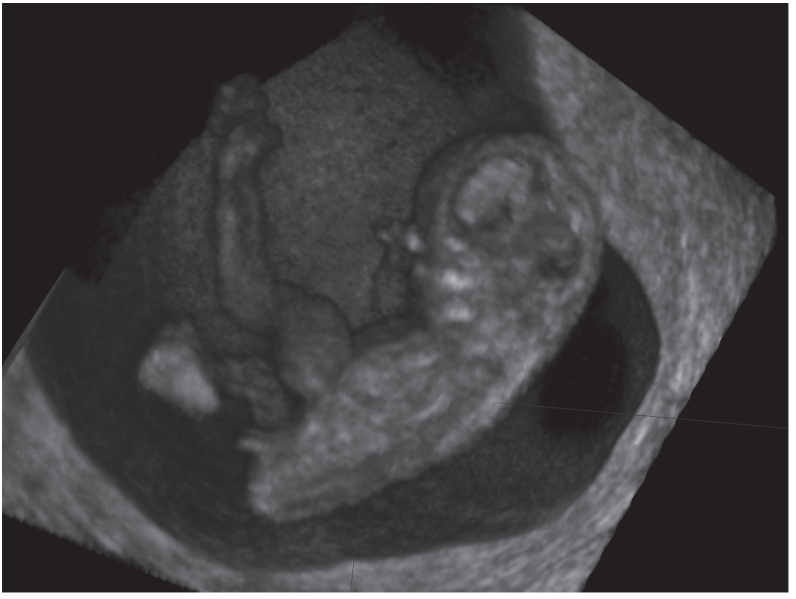

Figure 5: a pronounced genital tubercle in a female foetus at a GA of 10 weeks and 2 days in the BARCO I-Space

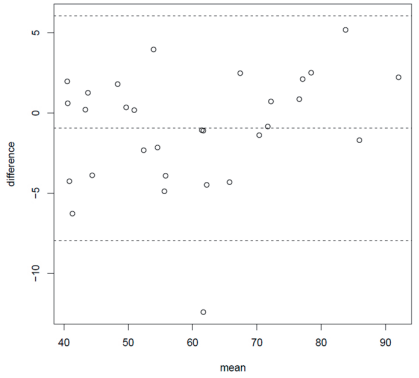

Figure 6: Bland and Altman plot for intrarater agreement
Data shown are the differences (second minus first) of measured genital tubercle angles of one rater plotted against the mean of the two measurements. The dashed outer lines show the 95% limits of agreement (LOAs), the dashed middle line represents the mean difference

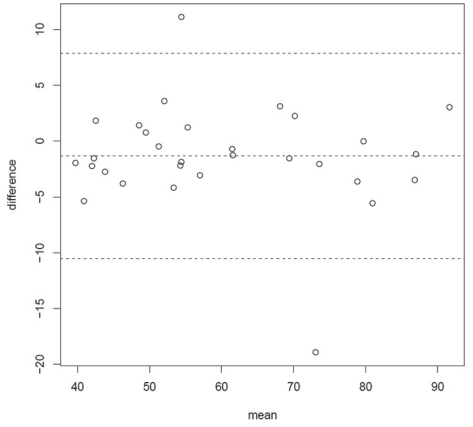

Figure 7: Bland and Altman plot for interrater agreement
Data shown are interrater differences of measured genital tubercle angles plotted against the mean of the two rater measurements. The dashed outer lines show the 95% limits of agreement (LOAs), the dashed middle line represents the mean difference.

Most research on foetal sex prediction in the first trimester has been performed at the end of the first trimester. To the best of our knowledge, we are the first who investigated the possibilities of angle measurement and sex prediction before 11 weeks of pregnancy.

Trying to push the borders we employed the most advanced technique, namely the 3D VR approach. 3D VR is superior in very precise and accurate positioning of lines and it has already shown its benefits in examining surface abnormalities and the foetal genitalia.[10, 11] Although this system is not widely available, a desktop VR system has been developed with comparable 3D views, using polarising glasses and an optical tracking system, implementing the same 3D VR measurement tools. We used the CRL line instead of a line tangentially to most dorsal part of the body since the former can be drawn more precisely.

Until 11 weeks GA we could not find a difference in angles between male and female foetuses. From 11 weeks onwards, mean male angles start to increase whereas female angles still decrease, which might be caused by foetal erectile movements.[9] Hsiao et al. and Youssef et al. investigated the foetal sex from 11+0 until 13+6 weeks GA and found the success rate of correctly predicting the sex to increase with advancing GA.[3, 4] Efrat et al. investigated foetal sex prediction in 656 women and predicted this incorrectly in 8.5% of eventually female foetuses until 12+4 GA.[5] From 13+0 GA onwards, a success rate of 100% was achieved. Lower success rates were reported by Chelli et al: in 85.7% foetal sex prediction was accurate, yet in male foetuses an increase in the genital angle was observed with increasing CRL.[6] Also Michailidis et al. observed a lower correct prediction rate of the foetal sex in offline studying 3D volumes by two different examiners of 85.3%.[8] Mazza et al. concluded in their study of 2374 foetuses not to assign foetal sex below a biparietal diameter (BPD) of 22 mm (which equals 12+5 GA[17]). From that moment onwards, however, an accuracy rate of 99% was obtained.[7] Recently Manzanares et al. investigated between 11 and 14 weeks GA foetal sex prediction and factors influencing correct prediction. After excluding 6.5% of the foetuses in which an intermediate angle

(not sufficiently discriminating between sexes) was found, in the remaining foetuses an overall correct prediction rate of 87.5% was achieved. Correct prediction was positively correlated with GA and CRL and negatively with maternal BMI.[18]

In view of the huge overlap even at 13 weeks GA and the inability to predict foetal sex in individual cases, all these findings are in accordance with ours. Until about 13 weeks GA accuracy is low and after 13 weeks GA, the visibility of the difference between male and female angles increases with advancing GA. It is a limitation of our study that we have only data available until 13 weeks GA.

Another limitation is the low feasibility rate of angle measurement of 55.2%. The measurements however, were performed offline on stored data. The low feasibility figure is a result of non-targeted scanning, acoustic shadowing and movement artefacts. If it was possible to measure the angle, until 11 weeks GA foetal sex could not be predicted whereas from 11 to 13 weeks the angle measurement insufficiently discriminated between male and female foetuses. In all of these foetuses, in up to 23.0% it was not possible at all to predict foetal sex by looking at the appearance of the genitalia and, if prediction was possible, in at best half of the cases prediction was correct. This also means a warning for clinicians that a male appearance of a pronounced genital tubercle before 13 weeks GA is not unusual in female foetuses (**Figure 5**).

Also the distance between base of the genital tubercle and the caudal end of the foetus can be used to differentiate between foetal sex. In newborns in males this distance is twice as long as in females. This measurement has recently been described for the first time in pregnancies between 11 and 14 weeks GA but correct prediction differed between 64% and 100% depending on GA.[19]

A different non-invasive way of determining foetal sex is by obtaining cell-free foetal DNA in maternal blood by detecting DNA sequences of the Y

chromosome.[20] This technique has a proven sensitivity and specificity of 100% and it can already be performed in the first trimester of pregnancy, from 7 – 9 weeks GA onwards.[21, 22] This test is, although more cumbersome compared to bedside testing and more expensive, superior to ultrasonographic sex determination in this early stage.

Conclusion

Our results indicate that accurate determination of the foetal sex by genital tubercle angle measurement or looking at a male or female genital appearance in the first trimester of pregnancy is very limited, even by using very high quality 3D Virtual Reality ultrasound techniques. We therefore conclude that if foetal sex has to be determined other techniques like DNA sequencing should be used.

Acknowledgments

We would like to thank Erwin Birnie PhD and Sten P. Willemsen PhD for helping with the statistical analysis of the data.

References

1. Odeh M GV, Kais M, Ophir E, Bornstein J. Sonographic fetal sex determination. Obstet Gynecol Surv. 2009;64(1):50-7.
2. Sajjad Y. Development of the genital ducts and external genitalia in the early human embryo. J Obstet Gynaecol Res. 2010;36(5):929-37.
3. Youssef A, Arcangeli T, Radico D, Contro E, Guasina F, Bellussi F, et al. Accuracy of fetal gender determination in the first trimester using three-dimensional ultrasound. Ultrasound Obstet Gynecol. 2011;37(5):557-61.
4. Hsiao CH, Wang HC, Hsieh CF, Hsu JJ. Fetal gender screening by ultrasound at 11 to 13(+6) weeks. Acta Obstet Gynecol Scand. 2008;87(1):8-13.
5. Efrat Z, Perri T, Ramati E, Tugendreich D, Meizner I. Fetal gender assignment by first-trimester ultrasound. Ultrasound Obstet Gynecol. 2006;27(6):619-21.
6. Chelli D, Methni A, Dimassi K, Boudaya F, Sfar E, Zouaoui B, et al. Fetal sex assignment by first trimester ultrasound: a Tunisian experience. Prenat Diagn. 2009;29(12):1145-8.
7. Mazza V, Di Monte I, Pati M, Contu G, Ottolenghi C, Forabosco A, et al. Sonographic biometrical range of external genitalia differentiation in the first trimester of pregnancy: analysis of 2593 cases. Prenat Diagn. 2004;24(9):677-84.
8. Michailidis GD, Papageorgiou P, Morris RW, Economides DL. The use of three-dimensional ultrasound for fetal gender determination in the first trimester. Br J Radiol. 2003;76(907):448-51.
9. Pedreira DA, Yamasaki A, Czeresnia CE. Fetal phallus 'erection' interfering with the sonographic determination of fetal gender in the first trimester. Ultrasound Obstet Gynecol. 2001;18(4):402-4.
10. Baken L, Rousian M, Koning AH, Bonsel GJ, Eggink AJ, Cornette JM, et al. First-Trimester Detection of Surface Abnormalities: A Comparison of 2- and 3-Dimensional Ultrasound and 3- Dimensional Virtual Reality Ultrasound. Reprod Sci. 2014;21(8):993-9.
11. Verwoerd-Dikkeboom CM, Koning AH, Groenenberg IA, Smit BJ, Brezinka C, Van Der Spek PJ, et al. Using virtual reality for evaluation of fetal ambiguous genitalia. Ultrasound Obstet Gynecol. 2008;32(4):510-4.
12. Steegers-Theunissen RP, Verheijden-Paulissen JJ, van Uitert EM, Wildhagen MF, Exalto N, Koning AH, et al. Cohort Profile: The Rotterdam Periconceptional Cohort (Predict Study). Int J Epidemiol. 2016;45(2):374-81.

13. Knez J, Day A, Jurkovic D. Ultrasound imaging in the management of bleeding and pain in early pregnancy. Best Pract Res Clin Obstet Gynaecol. 2014;28(5): 621-36.

14. Verwoerd-Dikkeboom CM, Koning AH, Hop WC, Rousian M, Van Der Spek PJ, Exalto N, et al. Reliability of three-dimensional sonographic measurements in early pregnancy using virtual reality. Ultrasound Obstet Gynecol. 2008;32(7): 910-6.

15. Rousian M, Koning AH, van Oppenraaij RH, Hop WC, Verwoerd-Dikkeboom CM, van der Spek PJ, et al. An innovative virtual reality technique for automated human embryonic volume measurements. Hum Reprod. 2010;25(9):2210-6.

16. Landis JR, Koch GG. The measurement of observer agreement for categorical data. Biometrics. 1977;33(1):159-74.

17. Verburg BO, Steegers EA, De Ridder M, Snijders RJ, Smith E, Hofman A, et al. New charts for ultrasound dating of pregnancy and assessment of fetal growth: longitudinal data from a population-based cohort study. Ultrasound Obstet Gynecol. 2008;31(4):388-96.

18. Manzanares S, Benitez A, Naveiro-Fuentes M, Lopez-Criado MS, Sanchez-Gila M. Accuracy of fetal sex determination on ultrasound examination in the first trimester of pregnancy. J Clin Ultrasound. 2016;44(5):272-7.

19. Arfi A, Cohen J, Canlorbe G, Bendifallah S, Thomassin-Naggara I, Darai E, et al. First-trimester determination of fetal gender by ultrasound: measurement of the ano-genital distance. Eur J Obstet Gynecol Reprod Biol. 2016;203:177-81.

20. Wright CF, Chitty LS. Cell-free fetal DNA and RNA in maternal blood: implications for safer antenatal testing. BMJ. 2009;339:b2451.

21. Scheffer PG, van der Schoot CE, Page-Christiaens GC, Bossers B, van Erp F, de Haas M. Reliability of fetal sex determination using maternal plasma. Obstet Gynecol. 2010;115(1):117-26.

22. Colmant C, Morin-Surroca M, Fuchs F, Fernandez H, Senat MV. Non-invasive prenatal testing for fetal sex determination: is ultrasound still relevant? Eur J Obstet Gynecol Reprod Biol. 2013;171(2):197-204.

CHAPTER 6

Human embryonic curvature studied with 3D ultrasound in ongoing pregnancies and miscarriages.

Bogers H, Uitert EM van, Ginkel S van, Mooren EDH van der, Groenenberg IAL, Eilers PHC, Exalto N, Steegers EAP, Steegers-Theunissen RPM

Reprod Biomed Online. 2018 May;36(5):576-583.

Abstract

Embryonic growth is often impaired in miscarriages. We hypothesise that derangements in embryonic growth result in abnormalities of the embryonic curvature. This study aims to create first trimester reference charts of the human embryonic curvature and investigate differences between ongoing pregnancies and miscarriages.

Weekly ultrasonographic scans from ongoing pregnancies and miscarriages were used from the Rotterdam periconceptional cohort and a cohort of recurrent miscarriages. In 202 ongoing pregnancies and 33 miscarriages first trimester crown rump length and total arch length were measured to assess the embryonic curvature.

The results show that the total arch length increases and shows more variation with advanced gestation. The crown rump length / total arch length ratio shows a strong increase from 8^{+0} to 10^{+0} weeks and flattening thereafter. No significant difference was observed between the curvature of embryos of ongoing pregnancies and miscarriages. The majority of miscarried embryos could not be measured. Therefore, this technique is too limited to recommend the measurement of the embryonic curvature in clinical practice.

Introduction

Ultrasonographic parameters, such as the crown rump length (CRL), embryonic volume (EV), and description of the Carnegie Stages are available for the clinical and scientific evaluation of embryonic growth and development.[1-3] Recently, we demonstrated that human embryonic growth trajectories are associated with estimated foetal weight and birth weight.[1] Several periconceptional maternal conditions, such as the folate status, age, smoking and alcohol use contribute to embryonic growth and development, birth weight as well as to adverse pregnancy outcomes, e.g., neural tube defects and miscarriages.[4, 5]

Impaired embryonic growth is often observed in pregnancies ending in a miscarriage, whereby the frequency of neural tube defects is approximately 10-fold increased.[6, 7] From this background we hypothesise that impaired embryonic growth and development is associated with an abnormal embryonic curvature.

Our first aim was to study first trimester the human embryonic curvature and to create reference charts using a multivariate Bayesian model as has been developed by our group.[8] A second aim was to study differences in the embryonic curvatures between ongoing pregnancies and pregnancies ending in a miscarriage.

Materials and methods

This observational study is embedded in the Rotterdam periconceptional cohort (Predict study), an ongoing prospective cohort study conducted at the Erasmus MC, University Medical Centre, in Rotterdam, the Netherlands.[9] Pregnant women who participated in this study in 2009 and 2010 were enrolled via the outpatient clinic of the department of Obstetrics and Gynaecology at the Erasmus MC and local midwifery practices. Since 2003 as part of our routine clinical care women with a history of recurrent spontaneous miscarriage received biweekly ultrasound scans. We included a cohort of these women visiting our outpatient clinic between 2008 and 2015 for analysis.

The methods used were the same for both cohorts. All participants signed a written informed consent and the local medical ethics committee approved the study protocol (METC 232.394/2003/177 – 9 November 2005, METC 3232.395/2003/178 – 9 November 2005, MEC 2004–227 - 15 October 2004).

All women with ongoing pregnancies and those ending in a miscarriage received weekly 3D scans between 6^{+0} and 12^{+6} weeks gestational age (GA). Only women less than eight weeks pregnant entered the study and twins were excluded.

Ultrasonographic data

Transvaginal ultrasonographic volumes were obtained with Voluson E8 ultrasound equipment (GE Medical Systems, Zipf, Austria) using a transvaginal probe (GE-probe RIC-6-12-D; 4.5–11.9 MHz). With regard to the safety aspects of first trimester ultrasound the thermal index (TI) and mechanical index (MI) were kept below 1.0, the examiners were qualified and experienced, the duration of the examination did not exceed 30 minutes, the as low as reasonably practicable (ALARP) principle was respected and 3D images were stored for offline evaluation in order to reduce the exposure to ultrasound as much as possible.[10] The 3D volumes were evaluated offline by projecting these on the screen of the ultrasound machine and were displayed in the multiplanar mode for analysis. The images were rotated in order to obtain a precise midsagittal view of the embryo in the A-plane resulting in an axial view in the B- and a coronal view in the C-plane (**Figure 1**). The data were stored and all measurements were performed offline as recently described by our group.[8] In the midsagittal plane were measured both CRL, used in clinical practice as the greatest length of the embryo,[11] and the total arch length (TAL) defined as the dorsal contour traced from the cranial calliper of the CRL to the caudal calliper (**Figure 2**). The CRL/TAL ratio is supposed to represent the calculated estimate of the embryonic curvature. Two observers randomly performed the TAL measurements in triplicate. The mean of three measurements was used for further analysis.

In the ongoing pregnancies data on pregnancy course and outcome were obtained from medical records.

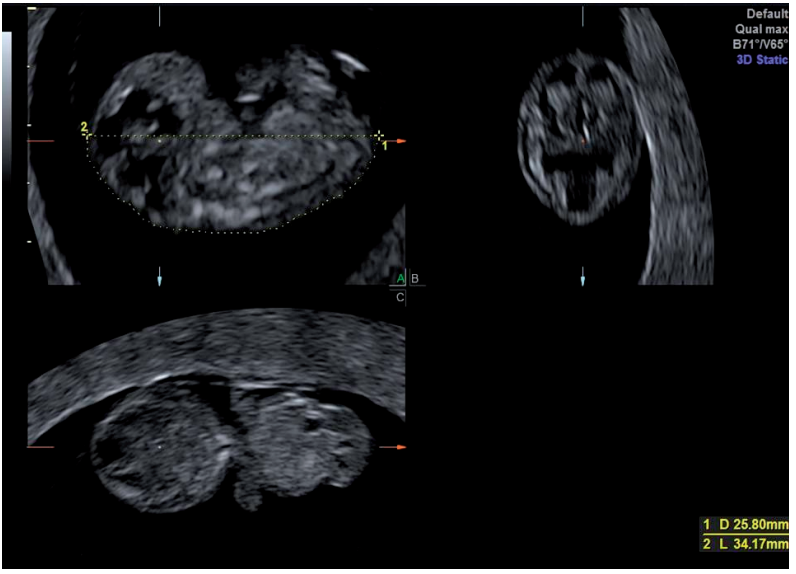

Figure 1: orthogonal triplanar image with crown rump length (CRL) and total arch length (TAL) measurements in the A-plane; A: sagittal view; B: axial view; C: coronal view

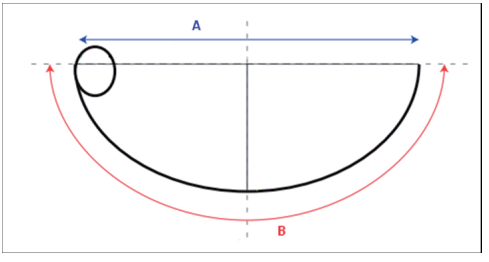

Figure 2: schematic representation of measurements; A: crown rump length (CRL), B: total arch length (TAL)

Pregnancy dating

According to our protocol, GA was calculated according to the first day of the last menstrual period when the woman had a regular cycle of 28±>3 days, we adjusted the GA for the duration of the menstrual cycle.[9] If the last menstrual period was missing or the difference of the GA determined by CRL and last menstrual period was more than 7 days, GA was based on the first CRL measurements after 8 weeks GA. In case of assisted reproductive technology, GA was determined by the date of oocyte retrieval plus 14 days in pregnancies conceived via in vitro fertilisation with or without intracytoplasmic sperm injection (IVF/ICSI), from the last menstrual period or insemination date plus 14 days in pregnancies conceived through intrauterine insemination, and from the day of embryo transfer plus 17 or 18 days in pregnancies originating from the transfer of cryopreserved embryos, depending on the number of days between oocyte retrieval and cryopreservation of the embryo.

Study population

From the Predict study we included 259 women enrolled in 2009 and 2010 (**Figure 3**) to create the reference charts of the embryonic curvature. We excluded one ectopic pregnancy, one pregnancy because of poor quality of the volumes, and 12 pregnancies with a discrepancy in GA of more than 6 days between CRL and the last menstrual period based on the Robinson curve or in case of an unknown last menstrual period. In the 245 pregnancies used for analysis we observed 43 miscarriages defined as a foetal death < 16 weeks GA. The 43 miscarriages from the Predict study were added to the 58 miscarriages derived from the recurrent miscarriage cohort, resulting in a total of 101 miscarriages. From this miscarriage cohort we had to exclude 9 pregnancies in which no images were obtained, 9 pregnancies with an empty sac and 50 pregnancies because of an early foetal demise resulting in a too small CRL for a precise TAL measurement. Of the resulting 33 miscarriages available for further analysis, 15 occurred after a history of recurrent miscarriages, defined as three or more miscarriages.

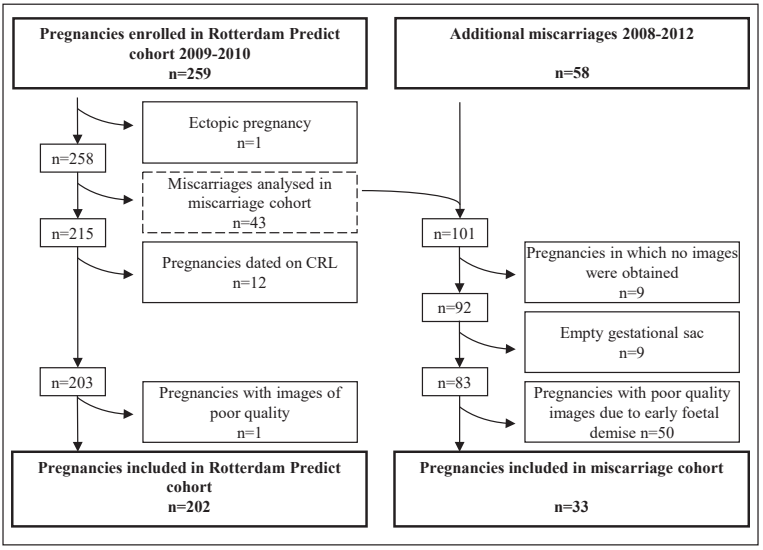

Figure 3: flowchart of study population

Statistical analysis

Maternal and pregnancy characteristics were summarised for the Predict cohort and the miscarriage cohort and compared between groups using the χ^2-test for categorical data, Student's *t*-test for normal distributions and the Mann-Whitney U-test for nonparametric continuous data.

Computations were performed with SPSS20 (IBM inc., Armonk, NY, USA) and R (R Foundation for Statistical Computing, Vienna, Austria). The standard deviation (SD) curves in **Figure 7** were computed with the R package gamlss,[12] assuming a model with a normal distribution, without transformation, and a spline for the mean curve and a linear relationship between the logarithm of the SD and GA.[8] The graph in **Figure 8** was made with the package ggplot2.

Reproducibility

The measurements of both CRL and TAL in the same volume were independently repeated three times and mean values were used for analysis. To assess intra- and interobserver reproducibility, a randomly selected subset of 30 first trimester volumes from 30 randomly selected pregnancies from the Predict cohort was measured a second time by the same examiner (SvG) and independently by another examiner (EvdM). For this purpose, five volumes were selected from each gestational week. Both examiners were blinded to the results of each other's measurements, each volume was unadjusted (raw data) and each measurement required manual adjustment of the volume to obtain the right image.

Results

General characteristics of ongoing pregnancies and miscarriages are shown in **Table 1**. In both groups the mean age (years ±SD) was comparable (32.1 ± 4.8 vs 33.7 ± 5.3 years respectively; P = 0.08). There was no significant difference between the groups in the number of women who were nulliparous (61.4% vs 48.5% respectively; P = 0.12) and conceived by means of in vitro fertilisation with or without intracytoplasmic sperm injection (30.7% vs 18.2% respectively; P = 0.14). In ongoing pregnancies after the first trimester, 5 (2.5%) pregnancies were terminated or ended in foetal or neonatal demise and 3 (1.5%) pregnancies resulted in a live born child with a congenital anomaly. Median GA at the moment of the first weekly visit was 7^{+0} (6^{+0} – 9^{+1}) in the ongoing pregnancy cohort and 6^{+5} (6^{+0} – 9^{+4}) weeks in the miscarriage cohort, with a median of 6 (range: 4-8) and 3 (range: 1-7) visits respectively per patient. We did not observe any neural tube defect in the study populations.

In 202 ongoing pregnancies and 33 miscarriages, a total of 1294 and 97 3D scans were performed respectively, of which in 1010 (78.1%) and 63 (64.9%) volumes, respectively, the image quality was sufficient to perform the measurements for the embryonic curvature. The median number of

		Predict cohort		Miscarriages		P
		(n=202)	Missing	(n=33)	Missing	
Maternal age, in years		32.1 ± 4.8	9	33.7 ± 5.3	0	0.08
Nulliparous		124 (61.4)	5	16 (48.5)	0	0.12
Conception via IVF/ICSI		62 (30.7)		6 (18.2)	0	0.14
Pregnancy outcome			0		0	
	Miscarriage	-		33 (100.0)		
	Termination of pregnancy	2 (1.0)		-		
	Intra-uterine foetal death (>16wks)	2 (1.0)		-		
	Neonatal death	1 (0.5)		-		
	Livebirth	197 (97.5)		-		
Gestational age at delivery, in weeks^{+days} median (range)						
	All pregnancies	39+3 (14^{+3} – 42^{+0})	1	-		
	>24 weeks	39+3 (27^{+0} – 42^{+0})	0	-		
Birth weight (>24wks), in g		3305 ± 554	0	-		
Infant sex, male		95 (47.3)	1	-		
Congenital anomaly				-		
	All pregnancies	6 (3.0)	1			
	Livebirths	3 (1.5)	0			

Table 1: general characteristics of the Predict cohort and miscarriages included for the analysis, numbers are n(%) or mean ± standard deviation unless otherwise specified; IVF/ICSI, in vitro fertilisation with or without intracytoplasmic sperm injection

volumes in which we could measure the curvature was 5 (range: 2-7) in ongoing pregnancies and 1 (range: 1-5) in miscarriages. The reproducibility of the embryonic curvature is shown in **Table 2** and **Figure 4**. All intraclass correlation coefficient (ICC) values of inter- and intraobserver agreement were above 0.997, representing excellent reliability of the measurements between and within the two operators (**Table 2**). The Bland-Altman plots showed good agreement between the measurements as well (**Figure 4**).

In **Table 3** we illustrate that the percentages of ultrasound volumes in which the measurements for the curvature could be performed varied with GA. Between 8 and 11 weeks, more than 90% of volumes could be measured,

	Mean difference (%)	SD	ICC
Intra observer variability			
CRL	0.34	1.47	0.999
TAL	2.66	3.11	0.998
Inter observer variability			
CRL	-0.24	2.23	0.999
TAL	-0.05	4.31	0.997

Table 2: reproducibility of crown-rump length (CRL) and total arch length (TAL) measurements; ICC, intraclass correlation coefficient; SD, standard deviation

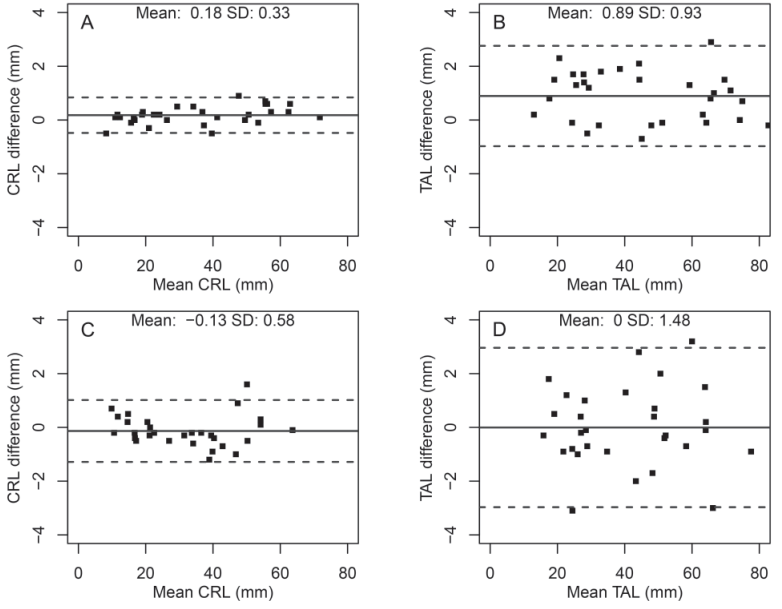

Figure 4: Bland-Altman plots of the intraobserver (upper figures) and interobserver (lower figures) variability for crown-rump length (CRL) and total arch length (TAL) measurements; SD = standard deviation

Week	All pregnancies (n=235)	%	Ongoing pregnancies (n=202)	%	Miscarriages (n=33)	%
6	34/141	24.1	32/127	25.2	2/14	14.3
7	132/207	63.8	117/178	65.7	15/29	51.7
8	195/214	91.1	175/190	92.1	20/24	83.3
9	188/202	93.1	174/186	93.5	14/16	87.5
10	179/191	93.7	174/185	94.1	5/6	83.3
11	165/191	86.4	161/187	86.1	4/4	100.0
12	138/182	75.8	136/179	76.0	2/3	66.7

Table 3: success percentages of total arch length measurements (measurements/ number of images; %) by gestational age (expressed in complete weeks)

whereas at 6 and 7 weeks this was only possible in 24% and 64% respectively. After 12 weeks, this percentage dropped to 76%.

Figure 5 shows the relation between TAL and GA. TAL increased and showed more variation with increasing GA. The relation between TAL and CRL is

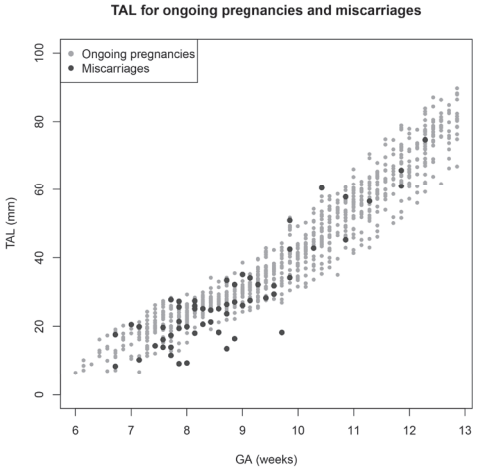

Figure 5: total arch length (TAL) versus gestational age (GA) for ongoing pregnancies and miscarriages

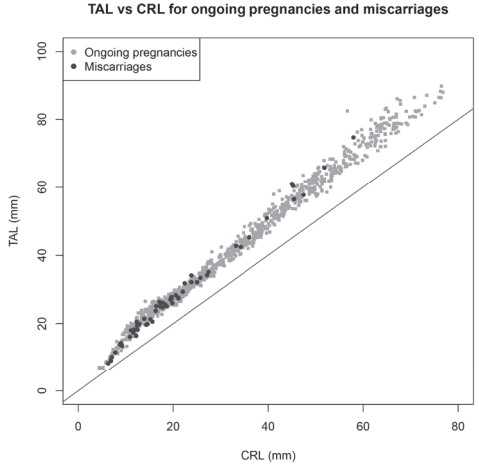

Figure 6: total arch length (TAL) versus crown rump length (CRL) for ongoing pregnancies and miscarriages

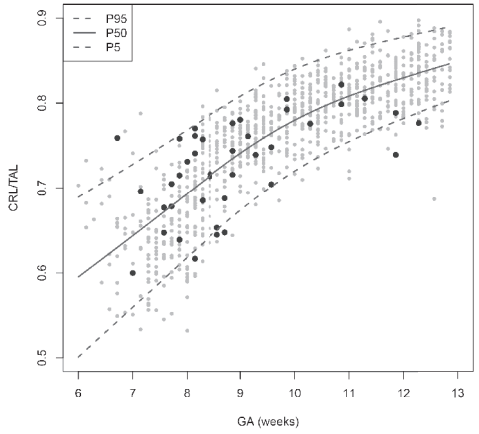

Figure 7: reference chart with percentile lines of the crown rump length crown rump length / total arch length ratio (CRL/TAL) versus the gestational age (GA); grey dots: ongoing pregnancies, black dots: miscarriages

shown in **Figure 6**. The CRL/TAL ratio represents the calculated estimate of the embryonic curvature. **Figure 7** displays the CRL/TAL ratio versus GA as reference chart, including percentile lines. The CRL/TAL ratio shows a strong increase at the beginning of the curve from 8^{+0} to 10^{+0} weeks, after which the curve flattens. This indicates that the embryo, being almost a circle in the very early stages, is gradually coming in a more linear, uncurved position mainly between 8 and 10 weeks GA. Longitudinal charts of the individual curvature of miscarriages are shown in **Figure 8**. No significant differences were observed in TAL and CRL/TAL between ongoing pregnancies and miscarriages.

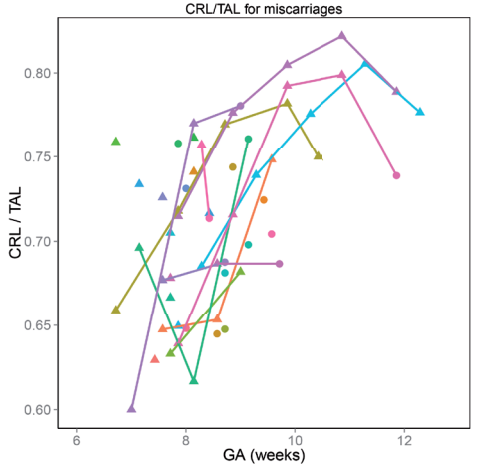

Figure 8: crown-rump length / total arch length ratio (CRL/TAL) versus gestational age (GA) plotted for individual miscarriages; triangles represent measurements in embryos with positive heart action and circles were used for measurements after embryonic demise

Discussion

In this prospective periconception cohort we have created reference charts of the human embryonic curvature in the first trimester of pregnancy in a study population derived from a tertiary care outpatient clinic. The data were analysed by means of a novel multivariate Bayesian model for longitudinal measurements.[8] This tailor made model provided a better fit than the existing univariate model.

We demonstrated that the first trimester curvature of the human embryo could be estimated reliably by measuring the CRL and TAL and calculating the CRL/TAL ratio. The embryonic curvature is positively associated with CRL and GA and decreases towards the end of the first trimester. Significant differences of the CRL/TAL ratio between miscarriages and ongoing pregnancies were not observed. Since we are the first to measure the curvature in both ongoing pregnancies as well as miscarriages, it will be difficult to estimate how many pregnancies ending in a miscarriage should be measured in order to observe a difference. Although we obtained volumes in 92 pregnancies ending in a miscarriage, the low feasibility in the miscarriage cohort precludes us from drawing firm conclusions. Therefore, the technique is too limited to recommend the measurement of the embryonic curvature and cannot be applied to the majority of women experiencing a miscarriage.

From studies on embryonic development it is known that the curved shape at about 7 weeks GA changes to an upright position at about 10 weeks.[11] This straightening mechanism, most likely caused by differences in growth rate of several embryonic structures, will influence the CRL measurement, as it is generally accepted to measure the greatest length in a straight line for this growth parameter. These changes are supported by our data, in which we observed a decrease in curvature in this period (**Figure 7**).

First trimester embryonic measurements are strongly determined by GA.[13] In order to reduce confounding by imprecise dating we therefore excluded pregnancies with a discrepancy in GA of more than 6 days between CRL and

the last menstrual period. The repeated measurements were performed on ultrasound scans obtained between 6^{+0} to 12^{+6} weeks GA. The feasibility of the measurements appeared to be best between 8 to 11 weeks GA. The problems of imprecise measurements before 8 weeks and after 12 weeks appeared to be due to the small size of the embryos and the increasing artefacts due to foetal movements, respectively. No difference in embryonic curvature could be observed between ongoing pregnancies and pregnancies ending in a miscarriage, which might be due to the small number of miscarriages in which measurements could be performed.

Prenatal detection of congenital anomalies is gradually shifting to the late first trimester. The intracranial translucency and other signs and ratios in the first-trimester posterior brain have been used for the detection of spina bifida.[14] In this study, as a first step the feasibility of the estimation of the embryonic curvature is demonstrated. This might be of particular interest for the screening of specific anomalies of the spinal column, including neural tube defects, such as spina bifida at an even earlier stage. Prenatal detection of neural tube defects will depend on the type of the anomaly and the GA. We can only speculate about the question whether the CRL/TAL ratio in the future may contribute to an earlier detection of spina bifida, which in current clinical practice is diagnosed mostly in the second trimester of pregnancy.[15]

In mice, the *curly tail* (*ct*) mutation is associated with spina bifida. It is not clear whether the increased curvature associated with failure of closure of the posterior neuropore is the cause or consequence of the spina bifida aperta.[16] In other species, including man, a decreased curvature was related to an increase in closure of the posterior neuropore.[17]

We were not able to study possible changes in the curvature in association with neural tube defects, since we did not observe any neural tube defects sonographically and pathological examination of miscarriage tissue was not available. However, it would be interesting to further investigate the embryonic curvature with CRL and TAL measurements in spina bifida and other

spinal column related anomalies in a large first trimester birth cohort with the pathological investigation of miscarriage tissues and stillbirths in the future.

This will also give opportunities to investigate associations between periconceptional maternal conditions, such as folic acid supplement use, and the development of the embryonic curvature.

In conclusion, the curvature of the first trimester human embryo can be determined reliably using 3D ultrasound measurements for CRL and TAL and by calculating the CRL/TAL ratio with an optimal time window of 8 to 12 weeks GA. The curvature of embryos resulting in a miscarriage was not significantly different from ongoing pregnancies. Our charts might be used in further studies on embryonic growth or on development of first trimester prenatal diagnosis of anomalies related to the spinal column.

References

1. van Uitert EM, Exalto N, Burton GJ, Willemsen SP, Koning AH, Eilers PH, et al. Human embryonic growth trajectories and associations with fetal growth and birthweight. Hum Reprod. 2013;28(7):1753-61.
2. Verwoerd-Dikkeboom CM, Koning AH, Hop WC, van der Spek PJ, Exalto N, Steegers EA. Innovative virtual reality measurements for embryonic growth and development. Hum Reprod. 2010;25(6):1404-10.
3. Rousian M, Hop WC, Koning AH, van der Spek PJ, Exalto N, Steegers EA. First trimester brain ventricle fluid and embryonic volumes measured by three-dimensional ultrasound with the use of I-Space virtual reality. Hum Reprod. 2013;28(5):1181-9.
4. van Uitert EM, Steegers-Theunissen RP. Influence of maternal folate status on human fetal growth parameters. Mol Nutr Food Res. 2013;57(4):582-95.
5. Steegers-Theunissen RP, Steegers EA. Embryonic health: new insights, mHealth and personalised patient care. Reprod Fertil Dev. 2015.
6. Bottomley C, Daemen A, Mukri F, Papageorghiou AT, Kirk E, Pexsters A, et al. Functional linear discriminant analysis: a new longitudinal approach to the assessment of embryonic growth. Hum Reprod. 2009;24(2):278-83.
7. Philipp T, Kalousek DK. Neural tube defects in missed abortions: embryoscopic and cytogenetic findings. Am J Med Genet. 2002;107(1):52-7.
8. Willemsen SP, Eilers PH, Steegers-Theunissen RP, Lesaffre E. A multivariate Bayesian model for embryonic growth. Stat Med. 2015;34(8):1351-65.
9. Steegers-Theunissen RP, Verheijden-Paulissen JJ, van Uitert EM, Wildhagen MF, Exalto N, Koning AH, et al. Cohort Profile: The Rotterdam Periconceptional Cohort (Predict Study). Int J Epidemiol. 2016;45(2):374-81.
10. Knez J, Day A, Jurkovic D. Ultrasound imaging in the management of bleeding and pain in early pregnancy. Best Pract Res Clin Obstet Gynaecol. 2014;28(5):621-36.
11. O'Rahilly R, Muller F. Developmental stages in human embryos: revised and new measurements. Cells Tissues Organs. 2010;192(2):73-84.
12. Rigby RA, Stasinopoulos DM. Generalized additive models for location, scale and shape. J Roy Stat Soc C-App. 2005;54:507-44.
13. Papaioannou GI, Syngelaki A, Poon LC, Ross JA, Nicolaides KH. Normal ranges of embryonic length, embryonic heart rate, gestational sac diameter and yolk sac diameter at 6-10 weeks. Fetal Diagn Ther. 2010;28(4):207-19.

14. Maruotti GM, Saccone G, D'Antonio F, Berghella V, Sarno L, Morlando M, et al. Diagnostic accuracy of intracranial translucency in detecting spina bifida: a systematic review and meta-analysis. Prenat Diagn. 2016;36(11):991-6.

15. Cameron M, Moran P. Prenatal screening and diagnosis of neural tube defects. Prenat Diagn. 2009;29(4):402-11.

16. van Straaten HW, Copp AJ. Curly tail: a 50-year history of the mouse spina bifida model. Anat Embryol (Berl). 2001;203(4):225-37.

17. Peeters MC, Hekking JW, Shiota K, Drukker J, Van Straaten HW. Differences in axial curvature correlate with species-specific rate of neural tube closure in embryos of chick, rabbit, mouse, rat and human. Anat Embryol (Berl). 1998; 198(3):185-94.

CHAPTER 7

General discussion

The studies in this thesis present ultrasonographic evaluation and documentation of various physiological changes during early human development, being necessary for appropriate first trimester diagnostic procedures. Detailed knowledge on normal anatomy and physiology is essential to recognise pathology. In this thesis some morphological changes during organogenesis are studied. The developing organ systems studied were selected because of questions raised during clinical first trimester two-dimensional (2D) and three-dimensional (3D) ultrasound. These specific questions are described in the research objectives defined in the introduction to this thesis. The answers to these questions, although not all of them immediately applicable for clinical purposes, may serve as a background for attempts to improve first trimester detection of congenital anomalies in the near future.

Early diagnosis

The trend towards early sonographic screening for detection and diagnosis of structural anomalies is in line with other trends in obstetrics and prenatal diagnosis. For instance, the detection of cell free foetal deoxyribonucleic acid (DNA) in maternal blood provides the possibility of non-invasive diagnosis of chromosomal abnormalities at an early gestational age. First trimester biomarkers and uterine artery Doppler measurements are used to determine the risk of placental disorders like foetal growth restriction and pre-eclampsia later on in pregnancy. Early diagnosis and risk assessment offers physicians more time for counselling or to run additional confirmatory tests. In case of a congenital anomaly more time will become available for patients to take all treatment options into consideration, including termination of pregnancy. This is especially important in countries having gestational age related legal restrictions for termination of pregnancy, to avoid extrajudicial abortion.

There is another important, potentially beneficial, aspect of prenatal examination in the first trimester. Ultrasonographic visualisation improves significantly by using high frequency vaginal ultrasound probes as compared to low frequency abdominal probes, used in the second trimester. With vaginal ultrasound there is less interference of fat tissue and therefore less

absorption of ultrasound. However high frequency, resulting in high resolution, is associated with a decreased penetration of ultrasound resulting in a smaller scanning area. Vaginal ultrasound is therefore only suitable for first trimester ultrasound and not for routine second trimester ultrasound. A shorter duration of the investigation time, as a result of improved image quality, and an intensity reduction of the ultrasound energy, as a result of a shorter distance between the transducer and the embryo, both contribute to a reduced exposure time. Off-line examination of 3D and 3D virtual reality (3D VR) images furthermore reduces the exposure time and contribute to a safer procedure. It should be noted, though, that as long as low-intensity imaging is used and examiners adhere to the aforementioned ALARP-rule there is no scientific proof that sonography could be harmful in early pregnancy. The same applies to 3D ultrasound.[1]

There is a potential danger that the details observed during vaginal ultrasound by the clinician are not always understood and may lead to misinterpretation of normal morphology during normal embryonic development. This consideration necessitates more studies like the ones described in this thesis: research concerning normal foetal development during the first trimester.

Improving test characteristics

Increasing knowledge on first trimester ultrasound appearance of first trimester embryonic structures will improve the test characteristics by reducing the number of false positive and false negative findings. Our data may help in the prevention of both false positive and negative diagnoses in early pregnancy.

Relatively little is known about precise ultrasonographic details of first trimester brain development. We created size charts of the walls of the telencephalon, diencephalon and mesencephalon, which may help in diagnosing abnormal development of the central nervous system already in a very early stage of pregnancy (chapter 2).

Knowing the normal appearance and seize of a physiological omphalocoele (chapter 3) is very helpful in avoiding the wrong diagnosis of a pathological first trimester exomphalos. Using 3D VR we are the first to add the third dimension, yielding size charts of the volume of the omphalocoele as well.

The exact mechanism causing congenital clubfeet is still unknown. We confirmed in vivo a transient clubfoot stage in the development of the lower limb at 10-11 weeks gestational age (chapter 4). Our data may support further research on the aetiology of this relatively common anomaly.

The determination of the foetal sex in an early stage of pregnancy may be important in inheritable diseases. We showed that the determination of foetal sex should not be performed sonographically in the first trimester. An accurate determination turned out to be not possible by both quantitative and qualitative means (chapter 5). Amplification of cell-free foetal DNA in maternal blood, however, is, although expensive, an excellent and almost 100% accurate alternative.

Embryonic curvature is inversely correlated with gestational age. We introduced a measurement for this characteristic of growth and development and created reference charts (chapter 6). These charts may help in research on neural tube defects and other spinal abnormalities, in which embryonic curvature might be compromised.

Precautions

There are nevertheless potential downsides to these new insights. Routine ultrasound in early pregnancy will not only reveal more anomalies but also at an earlier gestational age. Some of these pregnancies would have ended in a miscarriage anyway. This overdiagnosis may cause more anxiety in pregnant women.[2] On the other hand, these formerly unknown diagnoses could provide an opportunity for genetic testing and may help in preconception counselling for future pregnancies.

We should also be aware of the fact that every examination bears the risk of a false-positive diagnosis. Extra testing will probably yield more false-positive findings. Even in case subsequent sonography appears to be normal, distress in future parents has already been initiated. It is therefore necessary that future parents are thoroughly counselled beforehand about the possibility of false-positive findings.[2]

Future

Although the new techniques have been proven to be useful, especially during the first trimester, conventional 2D imaging cannot just be replaced right now by 3D and 3D VR ultrasound. These new techniques, however, are already a useful help in diagnosis and counselling.

While 3D ultrasound is omnipresent in specialised centres for prenatal diagnosis, the possibility of performing 3D VR is not. We developed a desktop version of the BARCO I-Space with comparable VR imaging, using polarising glasses and a joystick, including the same 3D VR measurement tools.[3] We expect that with this simplified technical improvement, also resulting in a substantial reduction of acquisition costs, the 3D VR technique will become available as a built-in application in ultrasound equipment in the near future.

For some congenital anomalies, routinely detected in the second trimester, the question remains whether these can be detected in an earlier stage. Future research is necessary to find a reliable answer to this question for much more anomalies than studied in this thesis. For this type of research routinely stored first trimester 3D volumes are utmost important for creating the opportunity for looking back to observe if the particular abnormality was already present in the first trimester or not. Also, since most anomalies are nowadays diagnosed in the second trimester by means of 2D ultrasound, the cost and time efficiency of 3D imaging and of first trimester sonography has yet to be determined.

Conclusion

3D sonography and 3D VR enable us to gain new insights in physiological early human development and may improve diagnostics. If used prudentially, these techniques will probably show its many benefits in future.

References

1. Knez J, Day A, Jurkovic D. Ultrasound imaging in the management of bleeding and pain in early pregnancy. Best Pract Res Clin Obstet Gynaecol. 2014;28(5): 621-36.

2. Health Council of the Netherlands. Population Screening Act: first trimester scan for prenatal screening. The Hague: Health Council of the Netherlands, 2014; publication no. 2014/31.

3. Baken L, van Gruting IM, Steegers EA, van der Spek PJ, Exalto N, Koning AH. Design and validation of a 3D virtual reality desktop system for sonographic length and volume measurements in early pregnancy evaluation. J Clin Ultrasound. 2015;43(3):164-70.

CHAPTER 8

Summary/Samenvatting

Summary

Chapter 1 presents the introduction to this thesis. The structural anomaly scan is traditionally scheduled in the second trimester of pregnancy. Better understanding of early development and novel techniques results in shifting of prenatal screening and diagnosis to the first trimester. Due to the many changes observed in the foetus in early pregnancy, a thorough knowledge of this is necessary to discriminate between normal and abnormal findings. Innovative techniques like three-dimensional (3D) ultrasound and 3D virtual reality can be helpful tools in this early prenatal diagnosis. The aim of this thesis was to obtain a better understanding of physiological developmental changes of the foetus during the first trimester by using these innovative ultrasound techniques.

Compared with other organ systems, relative little is known about cerebral development in utero. Chapter 2 describes the development of the secondary brain vesicles telencephalon, diencephalon and mesencephalon. Between seven and thirteen weeks gestational age (GA) the thickness of these structures was measured by means of 3D ultrasound. It was feasible to create growth curves out of these measurements, which could be used for future research on congenital anomalies of the central nervous system and influences of environmental exposures.

In the first trimester the midgut temporarily protrudes in the umbilical cord, which is known as the physiological midgut herniation. Its dimensions, including volume measurements, are described in chapter 3. The umbilical cord was examined by means of 3D virtual reality between six and thirteen weeks GA and most of the midgut herniations appeared to be present during the 9th and 10th week of pregnancy. The reference curves created might be used in the future to distinguish a physiological midgut herniation from a pathological exomphalos (omphalocoele), a congenital anomaly in which the small intestine and sometimes even liver and gall bladder bulge into the umbilical cord.

In chapter 4 the development of the foetal foot position is discussed. In vitro research on the development of the lower limbs has already shown that the feet temporarily attain a club foot position during organogenesis. Using 3D virtual reality and an innovative measuring technique we demonstrated this transient club foot position in vivo as well. Between eight and thirteen weeks GA the foot position was measured and at ten and eleven weeks GA a physiological club foot was observed. The reference curves created with these measurements might be used in future to - perhaps already at the end of the first trimester – diagnose a pathological club foot (pes equinovarus). This is a congenital anomaly of the foot position in which the lower limb resembles a golf club.

Foetal sex prediction is not only performed for medical reasons but also at the request of the future parents. Chapter 5 describes the results of foetal sex prediction between nine and thirteen weeks GA. By means of virtual reality the angle between the genital tubercle and the body axis was measured in order to predict the foetal sex. Also the aspect of the external genitals was examined to predict foetal sex. Though regression analysis showed a difference between male and female curves, due to significant overlap of the individual measurements it was not feasible to reliably predict foetal sex. Prediction by means of examining the aspect of the genitalia appeared not be possible either.

Chapter 6 describes the results of the examination on the foetal curvature along the longitudinal axis. Using 3D ultrasound between six and thirteen weeks GA the curvature was determined, which was defined as the ratio of the length of the back of the foetus (total arch length) and the crown-rump length. The curvature appeared to diminish with advancing GA and reference curves were made.

Because early growth restriction can be a feature of an imminent miscarriage the curvature was also measured in a cohort of foetus resulting in a miscarriage. Yet, no difference in curvature was seen between ongoing pregnancies and miscarriages.

In chapter 7 the implications of the results and suggestions for future research are discussed. Prenatal diagnosis early in pregnancy not only provides more time for confirmatory tests, but has also advantages in imaging because high resolution ultrasound probes can then be used. Through the results of this thesis we gained more insight in normal development in early pregnancy which should result in less false positive as well as false negative diagnoses. One should however be cautious for disadvantages of this extra and early testing, e.g., overdiagnosis. It also remains to be determined if testing in the first trimester, and, if so to what extent, can replace second trimester testing. Future research on this and on the use of 3D ultrasound and virtual reality should be performed.

Samenvatting

Hoofdstuk 1 is de inleiding van dit proefschrift. Echoscopisch onderzoek in de zwangerschap om aangeboren afwijkingen op te sporen wordt doorgaans in het tweede trimester verricht. Door nieuwe inzichten en verbeterde technieken schuift dit onderzoek steeds meer op naar het eerste trimester van de zwangerschap. Vanwege de vele veranderingen die de foetus vroeg in de zwangerschap ondergaat is het noodzakelijk te beschikken over gedetailleerde kennis daarvan teneinde fysiologie van pathologie te kunnen onderscheiden. Vernieuwende technieken zoals driedimensionale (3D) echoscopie en 3D virtuele werkelijkheid kunnen hier een belangrijke rol bij spelen. Het doel van dit onderzoek was om de normale, fysiologische veranderingen van de zich ontwikkelende foetus beter te begrijpen door gebruik te maken van vernieuwende technieken.

In vergelijking met andere orgaansystemen is betrekkelijk weinig bekend over de ontwikkeling van het centrale zenuwstelsel. In hoofdstuk 2 wordt de ontwikkeling van de secundaire hersenblaasjes telencephalon, diencephalon en mesencephalon beschreven. Tussen zeven en dertien weken zwangerschap werd de dikte van deze structuren met behulp van 3D echoscopie gemeten. Het bleek mogelijk om van deze metingen groeicurven te kunnen maken die in de toekomst gebruikt kunnen worden om verder onderzoek te verrichten naar aangeboren afwijkingen en eventuele effecten van omgevingsfactoren.

Tijdens de organogenese vindt de normale ontwikkeling van de middendarm gedeeltelijk in de navelstreng plaats, in de zogenaamde fysiologische navelbreuk of fysiologische herniatie (hernia umbilicalis). De dimensies hiervan - waaronder het volume - tussen zes en dertien weken zwangerschap worden beschreven in hoofdstuk 3. Bij negen en tien weken zwangerschap bleek de navelbreuk het meest zichtbaar. Met behulp van 3D virtuele werkelijkheid zijn referentiecurven opgesteld die in de toekomst wellicht gebruikt zouden kunnen worden om onderscheid te kunnen maken met een pathologische

navelbreuk (omphalokèle), waarbij na de geboorte darmen en soms ook andere organen buiten de buikholte in de navelstreng aanwezig zijn.

In hoofdstuk 4 wordt de ontwikkeling van de voetstand uiteen gezet. Uit onderzoek in vitro was al bekend dat tijdens de ontwikkeling van de onderste ledematen de voeten tijdelijk een klompvoetstand aannemen. Wij hebben met behulp van 3D virtuele werkelijkheid en een vernieuwende meetwijze deze tijdelijke klompvoetstand ook in vivo aangetoond. Tussen acht en dertien weken zwangerschap werd de voetstand gemeten en bij tien-elf weken zwangerschap bleek er sprake van een fysiologische klompvoet. Van de metingen zijn referentiecurven gemaakt die in de toekomst gebruikt zouden kunnen worden om mogelijk al aan het einde van het eerste trimester onderscheid te kunnen maken met een pathologische klompvoet (pes equinovarus), waarbij ook na de geboorte de voet een afwijkende stand heeft ten opzichte van het onderbeen.

Niet alleen om medische redenen maar vooral ook op verzoek van toekomstige ouders wordt geprobeerd het foetale geslacht steeds vroeger te bepalen. In hoofdstuk 5 worden de resultaten van de geslachtsvoorspelling tussen negen en dertien weken zwangerschap beschreven. Met behulp van 3D virtuele werkelijkheid werd de hoek die het tuberculum genitale met de lichaamsas maakt gemeten om op basis hiervan het geslacht te bepalen. Ook werd het aspect van de uitwendige geslachtsorganen gebruikt voor een voorspelling van het geslacht. Hoewel de regressieanalyse wel een verschil tussen mannelijke en vrouwelijke foetus aantoonde was het door de overlap van de metingen niet mogelijk om in individuele gevallen een betrouwbare voorspelling te doen en ook de kwalitatieve inschatting bleek onbetrouwbaar te zijn in deze periode van de zwangerschap.

In Hoofdstuk 6 worden de resultaten van het onderzoek naar de kromming van de lengteas van de foetus beschreven. Met 3D echoscopie werd tussen zes en dertien weken zwangerschapsduur de kromming gemeten die werd gedefinieerd als de verhouding tussen de lengte van de rug (totale booglengte) en de kruin-stuitlengte. Het bleek dat met een toename van de

zwangerschapsduur er sprake was van een afnemende kromming en hier werden referentiecurven van gemaakt.

Omdat groeistoornissen vaker worden gezien bij zwangerschappen die eindigen in een miskraam werd in een aparte groep miskramen de kromming ook gemeten. Er bleek geen verschil te zijn tussen de doorgaande zwangerschappen en de miskramen.

In hoofdstuk 7 worden de bevindingen in een breed kader geplaatst. Diagnostiek vroeg in de zwangerschap geeft niet alleen tijdswinst voor nader aanvullend onderzoek, maar kent ook voordelen door betere beeldvorming met hoogfrequente echoscopie die alleen op dat moment kan worden gebruikt. De resultaten van deze dissertatie geven meer inzicht in de normale ontwikkeling vroeg in de zwangerschap waardoor verkeerde diagnosen (fout-positieven) en onterechte geruststelling (fout-negatieven) minder vaak zullen plaatsvinden. Wel moet opgepast worden voor overdiagnostiek en medicalisering. Daarnaast zal moeten blijken of afwijkingen die nu in het tweede trimester kunnen worden opgespoord ook al vroeger in de zwangerschap even duidelijk zichtbaar zijn. Toekomstig onderzoek zal zich hierop moeten richten en op de rol die 3D echoscopie en 3D virtuele werkelijkheid hierbij kunnen spelen.

Appendices

List of PubMed publications

This thesis

- Bogers H, Baken L, Cohen-Overbeek TE, Koning AHJ, Willemsen SP, van der Spek PJ, Exalto N, Steegers EAP. Evaluation of First-Trimester Physiological Midgut Herniation Using Three-Dimensional Ultrasound. Fetal Diagn Ther. 2018 Aug 15:1-7. doi: 10.1159/000489260. [Epub ahead of print]

- Bogers H, van Uitert EM, van Ginkel S, van der Mooren EDH, Groenenberg IAL, Eilers PHC, Exalto N, Steegers EAP, Steegers-Theunissen RPM. Human embryonic curvature studied with 3D ultrasound in ongoing pregnancies and miscarriages. Reprod Biomed Online. 2018 May;36(5):576-583

- Bogers H, Rifouna MS, Koning AHJ, Husen-Ebbinge M, Go ATJI, Spek PJ van der, Steegers-Theunissen RPM, Steegers EAP, Exalto N. Accuracy of fetal sex determination in the first trimester of pregnancy using 3D virtual reality ultrasound. J Clin Ultrasound. 2018 May;46(4):241-246

- Gijtenbeek M, Bogers H, Groenenberg IAL, Exalto N, Willemsen SP, Steegers EAP, Eilers PHC, Steegers-Theunissen RPM. First trimester size charts of embryonic brain structures. Hum Reprod. 2014 Feb;29(2):201-7

Other manuscripts

- Hitzerd E, Bogers H, Kianmanesh Rad NA, Duvekot JJ. A viable caesarean scar pregnancy in a woman using a levonorgestrel-releasing intrauterine device: a case report. Eur J Contracept Reprod Health Care. 2018 Apr;23(2):161-163

- Boekhorst F, Bogers H, Martens JE. Renal pelvis rupture during pregnancy: diagnosing a confusing source of despair. BMJ Case Rep. 2015; pii: bcr2014208400

- Bogers H, Bos D, Schoenmakers S, Duvekot JJ. Postpandemic influenza A/H1N1pdm09 is still causing severe perinatal complications. Mediterr J Hematol Infect Dis. 2015 Jan 1;7(1):e2015007

- Bogers H, Boer K, Duvekot JJ. Complications of the 2009 influenza A/H1N1 pandemic in pregnant women in The Netherlands: a national cohort study. Influenza Other Respir Viruses. 2012 Sep;6(5):309-12

- Bogers H, Cohen-Overbeek TE, Go ATJI. Parvovirus B19 infection in pregnancy and amniocentesis. Prenat Diagn. 2011 Nov;31(11):1109; author reply 1110

- Bogers H, Exalto N, Cohen-Overbeek TE. Unusual fetal abdominal wall presentation mimicking an abdominal wall defect. J Clin Ultrasound. 2011 Sep;39(7):410-1

- Van den Berg TJ, Bogers H, Vriesendorp TM, Surachno JS, DeVries JH, Ten Berge IJ, Hoekstra JBL. No apparent impact of postoperative blood glucose levels on clinical outcome in kidney transplant recipients. Clin Transplant. 2009 Mar-Apr;23(2):256-63

Personal data

Born 24th June 1982 in Gouda, the Netherlands. After primary education (basisschool Maria Bernadette, Leidschendam) and finishing grammar school (gymnasium, Sint-Maartenscollege, Voorburg), I studied medicine at "Universiteit van Amsterdam", graduating in 2007. Subsequently, I worked as a physician at the department of obstetrics and gynaecology at Ikazia Ziekenhuis in Rotterdam. In 2009 I started as a sonographist at the department of obstetrics and gynaecology at Erasmus MC in Rotterdam and simultaneously did research, resulting in this thesis. Since 2013, I have been a trainee in obstetrics and gynaecology, working in Rotterdam at Maasstad Ziekenhuis and Erasmus MC.

PhD portfolio

Name PhD student: Hein Bogers
Erasmus MC Department: Obstetrics and Gynaecology,
division of Obstetrics and Prenatal Medicine
PhD period: 2009-2018
Promotors: Prof Dr EAP Steegers and Prof Dr PJ van der Spek
Supervisors: Dr N Exalto and Dr AJH Koning

1. PhD training	**workload (ECTS)**
General courses	
• Jan 2010 biostatistics for clinicians, NIHES, Rotterdam	1.0
Specific courses	
• 5 - 6 Feb 2010 course on congenital anomalies and foetal echocardiography, London	0.5
• 1 Dec 2009 certificate of competence 'The 20-22 weeks scan' obtained, Fetal Medicine Foundation	4.0
• 17 Nov 2009 course on foetal echocardiography, Amsterdam	0.5
Presentations at national and international conferences	
• 21 June 2017 oral presentation weekly departmental scientific meeting	0.5
• 21 Oct 2016 oral presentation bimonthly educational meeting for specialist trainees, Rotterdam	0.5
• 1 Nov 2013 oral presentation scientific meeting Maasstad Ziekenhuis, Rotterdam	0.5
• 8 Feb 2013 oral presentation symposium jonge zwangerschap, Rotterdam	0.5
• 2 Dec 2011 oral presentation symposium jonge zwangerschap, Hoofddorp	0.5
• 20 Sep 2011 oral poster presentation ISUOG World Congress 2011, Los Angeles, CA	0.5
• 1 Dec 2010 oral presentation weekly departmental scientific meeting	0.5
• 10 Jun 2010 oral presentation scientific meeting Division of Prenatal Diagnosis	0.5

	workload (ECTS)
International conferences	
• 29 Jun - 3 Jul 2014 Fetal Medicine Foundation World Congress, Nice	1.0
• 18 - 22 Sep 2011 ISUOG World Congress 2011, Los Angeles, CA	1.0
• 10 - 11 Dec 2009 ESHRE campus 'early pregnancy winter course', Rotterdam	0.5
2. Teaching	
• 2010-2012 hands on-training masterclass Foetal Anomaly Scan for gynaecologists	1.5
• 2009-2012 teaching prenatal diagnosis to medical students, Erasmus Universiteit Rotterdam	4.0
• 2010 rewriting educational materials and exams of prenatal diagnosis for medical students, Erasmus Universiteit Rotterdam	1.0

Authors and affiliations

Erasmus MC, University Medical Centre Rotterdam, the Netherlands

from the Department of Obstetrics and Gynaecology, Division of Obstetrics and Prenatal Medicine:

- L Baken
- TE Cohen-Overbeek
- ATJI Go
- M Gijtenbeek
- N Exalto
- S van Ginkel
- IAL Groenenberg
- M Husen-Ebbinge
- EDH van der Mooren
- MS Rifouna
- EAP Steegers
- RPM Steegers-Theunissen
- EM van Uitert

from the Department of Bioinformatics:

- AHJ Koning
- PJ van der Spek

from the Department of Biostatistics:

- PHC Eilers
- SP Willemsen

Word of thanks

I owe many thanks to:

A Anton Koning, Attie Go

E Elisabeth van der Mooren, Eric Steegers, Erwin Birnie, Evelyne van Uitert

H Hans Kneefel

I Irene Groenenberg

L Leonie Baken

M Manon Gijtenbeek, Margreet Husen, Maria Rifouna

N Niek Exalto

P Paul Eilers, Peter van der Spek

R Régine Steegers-Theunissen

S Sharon van Ginkel, Sten Willemsen

T Tom de Vries Lentsch, Titia Cohen-Overbeek